

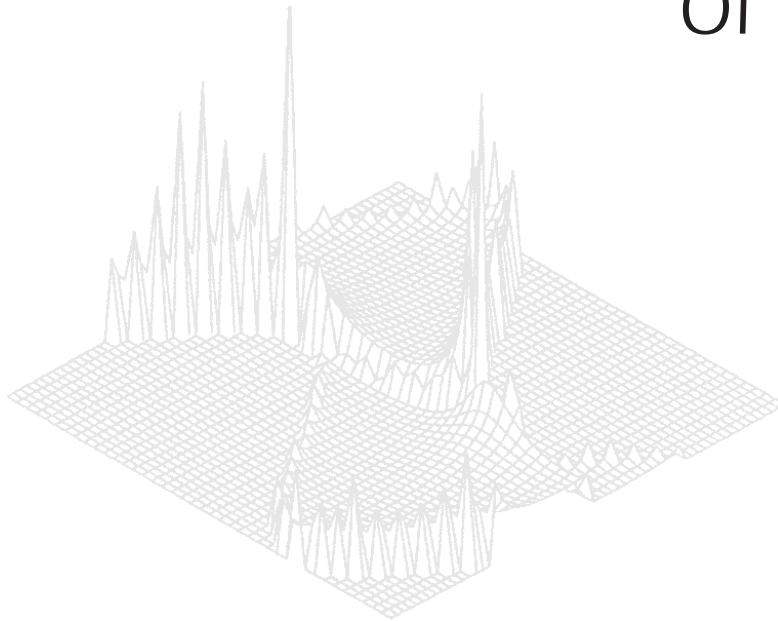
---

**C S I R O   P U B L I S H I N G**

---

# Australian Journal of Physics

Volume 51, 1998  
© CSIRO 1998



A journal for the publication of  
original research in all branches of physics

**[www.publish.csiro.au/journals/ajp](http://www.publish.csiro.au/journals/ajp)**

All enquiries and manuscripts should be directed to

*Australian Journal of Physics*

**CSIRO PUBLISHING**

PO Box 1139 (150 Oxford St)

Collingwood

Vic. 3066

Australia

Telephone: 61 3 9662 7626

Facsimile: 61 3 9662 7611

Email: [peter.robertson@publish.csiro.au](mailto:peter.robertson@publish.csiro.au)



Published by **CSIRO PUBLISHING**  
for CSIRO and the  
Australian Academy of Science



## A Review of the Low Temperature Properties of the Rare Earth Vanadates\*

*G. J. Bowden*

Department of Physics, University of Southampton,  
Highfield, Southampton S017 1BJ, UK.  
Permanent address: School of Physics, University of New South Wales,  
Sydney, NSW 2052, Australia.

### *Abstract*

The rare earth vanadates have long been studied for their interesting magnetic properties and cooperative Jahn–Teller distortions. In the main, most of this work has been carried out at temperatures down to 1 K or so (e.g. Gehring and Gehring 1975). In this review NMRON, and other low temperature experiments in the mK regime, are presented and discussed. It will be argued that the low temperature properties of these compounds are just as interesting as their high temperature counterparts. In general, the nuclear and electronic wavefunctions become intermixed, leading to a variety of interesting physical effects, such as enhanced nuclear magnetism, quadrupolar induced intermediate state re-orientation etc. These effects have, in turn, spawned new methods for the investigation of magnetic structures, and thermometric detection of NMR both by internal and external thermometers. Several experiments are suggested, including magnetic refrigeration, Mössbauer, EPR in the  $\approx 30$  GHz range, in addition to thermometric NMR and NMRON.

### 1. Introduction

Cooke *et al.* (1970, 1971) were the first authors to systematically probe the fascinating magnetic and optical properties of the rare earth (RE) vanadates. They showed that at 14 K  $\text{DyVO}_4$  undergoes a cooperative Jahn–Teller type crystallographic distortion, from tetragonal to orthorhombic, followed by a magnetic transition to an antiferromagnetic state at 3 K. This work was quickly complemented by extensive Raman scattering studies and theoretical work (e.g. Elliott *et al.* 1972), together with a plethora of experiments on other RE vanadates, phosphates and arsenates. For a summary of this early work the reader is referred to the comprehensive review by Gehring and Gehring (1975).

Since 1975 however, many new experiments have been performed on the vanadates. For example, Bleaney *et al.* (1981*a*, 1981*b*, 1982*a*, 1982*b*, 1982*c*, 1982*d*, 1982*e*) have made a special NMR study of the vanadates, using  $^{51}\text{V}$  as the NMR probe, at temperatures down to as low as  $\sim 0.48$  K. Still more recently, both neutron and electronic Raman scattering experiments (ERS) have been used to determine both crystal field levels for the RE ions, and electronic Raman transitions in several vanadates (e.g. Skanthakumar *et al.* 1995; Nguyen *et al.*

\* Refereed paper based on a contribution to the International Workshop on Nuclear Methods in Magnetism, held in Canberra on 21–23 July 1997.

1997). So it is fair to say that our current knowledge of the RE vanadates, at least above 1 K, has reached quite a sophisticated level.

In this review, a summary is given of the known properties of the RE vanadates. However, it should be stated at the outset that the primary focus of this review is on the properties of the RE vanadates below 1 K, where the nuclear hyperfine interaction begins to make its presence felt. For example, in  $\text{HoVO}_4$  the nuclear hyperfine interaction gives rise to the phenomenon of enhanced nuclear magnetism, where the  $^{165}\text{Ho}$  nuclear magnetic moments appear to be 170 times larger than normal. As a result  $\text{HoVO}_4$  enters a nuclear driven, antiferromagnetic state, in the mK regime (see for example Suzuki *et al.* 1978). This is some three orders of magnitude higher than that anticipated with bare (enhanced)  $^{165}\text{Ho}$  nuclear magnetic moments.

Since most of the low temperature properties of the vanadates have been extracted using nuclear magnetic resonance (NMR/NQR) or nuclear orientation (NO) studies, it will be assumed, for the purposes of this review, that the reader is familiar with the principles and applications of NMR, NQR, NO and NMRON (NMR on Oriented Nuclei), even though no NMRON results on the vanadates have been reported so far. The main references to NO and NMRON are Hamilton (1975) and Stone and Postma (1986). However, other introductions to NMRON have been given by BlinStoyle and Grace (1957), Stone (1989) and Lounasmaa (1974). In particular, Lounasmaa described how anisotropic  $\gamma$ -ray emission, from in situ radioactive  $^{60}\text{Co}$  in single crystal cobalt, can be used to determine temperatures in the mK range.

This review is set out as follows. In Sections 2 and 3, brief summaries of the known properties of the RE vanadates, and their hyperfine interactions, are presented and discussed. This is followed, in Sections 4 and 5, by a discussion of the known low temperature properties of  $\text{YbVO}_4$  and  $\text{HoVO}_4$ , respectively. The reasons underpinning this choice are: (i) these two compounds are representative of ground state Kramers doublet and non-magnetic singlet  $\text{RE}^{3+}$  ions, respectively, and (ii) their low temperature properties have been relatively well documented. In particular, these two compounds will be used to illustrate the new physics that has emerged from the NMRON experiments. Thereafter the remaining vanadates are discussed in turn, with the exceptions of  $\text{YVO}_4$  and  $\text{LuVO}_4$  which are essentially non-magnetic. In general, emphasis is placed on challenges that lie ahead.

No attempt is made to review the phosphates and the arsenates. While there are many similarities, there are also many differences. For example, in  $\text{HoVO}_4$  the ground state is a singlet with an excited state doublet at 2.4 meV ( $19.35\text{ cm}^{-1}$ ), whereas in  $\text{HoPO}_4$  the ground state is a doublet with a singlet at 8.4 meV ( $67.75\text{ cm}^{-1}$ ) (Skanthakumar *et al.* 1995). This change in ground state wavefunction has a profound effect on the low temperature magnetic properties of these two compounds.

## 2. Brief Review of the Properties of Vanadates above 1 K

As noted earlier, a review of the properties of the vanadates ( $\text{REVO}_4$ ), arsenates ( $\text{REAsO}_4$ ), phosphates ( $\text{REPO}_4$ ), and other compounds which exhibit cooperative Jahn–Teller effects, has been given by Gehring and Gehring (1975). However, for the purposes of this review, their known properties are briefly summarised below.

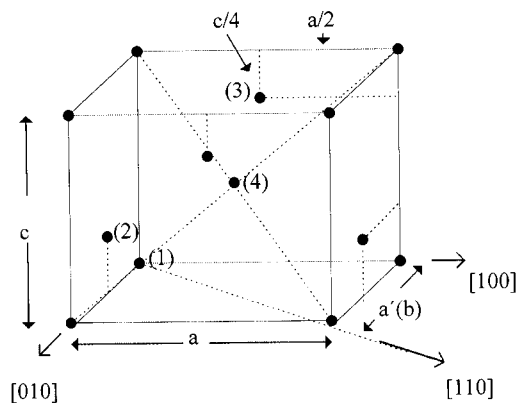


**Fig. 1.** Tetragonal zircon structure of the  $\text{REVO}_4$  vanadates. Only the RE ions are shown.

The vanadates crystallise in tetragonal zircon structure, space group  $I4_1/amd$  ( $D_{4h}^{19}$ ) (Wyckoff 1965), with point group symmetry  $D_{2d}$  at the RE site. The positions of the RE ions are shown in Fig. 1, which also illustrates the labelling convention adhered to in this review. The appropriate crystal field Hamiltonian for the  $\text{RE}^{3+}$  ion is given by

$$\mathcal{H}_{\text{CF}} = \theta_2 B_{20} O_{20} + \theta_4 (B_{40} O_{40} + B_{44}^c O_{44}^c) + \theta_6 (B_{60} O_{60} + B_{64}^c O_{64}^c), \quad (1)$$

where (i) the  $z$ -axis coincides with the  $c$ -axis of the crystal and (ii) the symbols in (1) possess their usual meanings (e.g. Hutchings 1965). However, the reader is warned that there are two crystal field formulations in the literature which can cause confusion. Wybourne (1965) has expressed the crystal field Hamiltonian in terms of unit spherical operators, which we write in the form:

$$\mathcal{H}_{\text{CF}} = \sum_{K,Q} \mathcal{B}_{KQ}^+ \theta_K \mathcal{C}_{KQ}, \quad (2)$$

where  $-K \leq Q \leq K$ . The relationship between the two sets of crystal field coefficients has been given by Kassman (1970):

$$\begin{aligned} \mathcal{B}_{20} &= 2B_{20}, & \mathcal{B}_{40} &= 8B_{40}, & \mathcal{B}_{60} &= 16B_{60}, \\ \mathcal{B}_{44} &= \frac{8}{\sqrt{70}} B_{44}^c, & \mathcal{B}_{64} &= \frac{8\sqrt{14}}{21} B_{64}^c. \end{aligned} \quad (3)$$

Since there is no possibility of confusion, we shall simply drop the upper suffix  $c$  when referring to the crystal field parameters  $B_{44}^c, B_{64}^c$ .

At lower temperatures, collective Jahn–Teller type distortions appear in some of the RE vanadates. There are two possible distortions, denoted by  $B_{1g}$  and  $B_{2g}$ , both of which lower the crystal symmetry from tetragonal to orthorhombic. In the case of the  $B_{1g}$  distortion, the  $a$ - $a'$  plane, originally square, becomes rectangular. Whereas for  $B_{2g}$ , the distortion takes place along a  $[110]$  or equivalent axis, turning the  $a$ - $a'$  plane into a rhombus. Thus the crystal field Hamiltonian of

(1) will have to be modified to take these distortions into account. The driving force behind both distortions is the lowering of the crystal field ground state of the  $\text{RE}^{3+}$  ion (first order in distortion), at the expense of the elastic energy stored in the lattice (second order in distortion). In this review article, special attention is given to the ground and first excited states of the RE ions, since it is these electronic states which are most affected by the presence of the nuclear hyperfine interactions.

**Table 1. Some properties of the  $\text{REVO}_4$  vanadates**

Compound	Néel temperature	Jahn–Teller distortion	Easy axis
$\text{YVO}_4$			
$\text{CeVO}_4$			
$\text{PrVO}_4$			$a$ - $a'$ plane
$\text{NdVO}_4$			$a$ - $a'$ plane
$\text{SmVO}_4$			
$\text{EuVO}_4$			
$\text{GdVO}_4$	$2.495 \text{ K}^{\text{E}}$		$c$ -axis
$\text{TbVO}_4$	$61(3) \text{ mK}^{\text{D}}$	$T_{\text{D}} = 33.1(1) \text{ K}^{\text{D}}$	[110]
$\text{DyVO}_4^{\text{A}}$	$3.066(2) \text{ K}$	$T_{\text{D}} = 14.0(5) \text{ K}$	$a$ -axis
$\text{HoVO}_4^{\text{C}}$	$4.8 \text{ mK}$	?	$a$ - $a'$ plane
$\text{ErVO}_4$	$0.4(1) \text{ K}^{\text{F}}$		$a$ - $a'$ plane
$\text{TmVO}_4^{\text{G}}$	$<100 \mu\text{K}^{\text{C}}$	$T_{\text{D}} = 2.1 \text{ K}$	$c$ -axis
$\text{YbVO}_4^{\text{B}}$	$93 \text{ mK}$		$c$ -axis
$\text{LuVO}_4$			

<sup>A</sup>Gehring and Gehring (1975); <sup>B</sup>Radhakrishna *et al.* (1981); <sup>C</sup>Suzuki *et al.* (1978); <sup>D</sup>Wells and Wornick (1972); <sup>E</sup>Cashion *et al.* (1970) and Metcalfe and Rosenberg (1972a); <sup>F</sup>Metcalfe and Rosenberg (1972b); <sup>G</sup>Suzuki *et al.* (1980).

Some of the principal properties of the RE vanadates, where they are known, are summarised in Table 1. In general, both the magnetic and structural transitions of the RE vanadates are determined primarily by the properties of the RE 4f electrons. For example, if the spin of the RE ion is integer, the vanadate in question may undergo a cooperative Jahn–Teller (CJT) distortion as the temperature is lowered. However, RE ions with half integer spins can also undergo CJT transitions, in special circumstances. Such a situation occurs in  $\text{DyVO}_4$  where two Kramers doublets form a near quartet ground state. On entering the CJT state, the energy of one of the Kramers doublet is depressed with respect to the other, thus providing the driving force for the transition.

### 3. Nuclear Properties of the Rare Earths

As the temperature is lowered below 1 K, the properties of the nuclei begin to make their presence felt through the magnetic and quadrupole hyperfine interactions. For convenience, the magnetic and quadrupole moments of the stable RE nuclei are summarised in Table 2.

In general, the largest contributors to the hyperfine interactions arise from intra-ionic coupling between the RE 4f electrons and the parent nucleus. Using the Wigner–Eckart theorem, it can be shown that the magnetic and quadrupole interactions take the form:

$$\mathcal{H}_{\text{M}} = A\mathbf{I} \cdot \mathbf{J}, \quad (4)$$

**Table 2. Stable nuclear moments in the RE series**

Taken from the CRC Handbook of Chemistry and Physics (76<sup>th</sup> Edition). Isotopes not shown have spin  $I = 0^+$ . This includes all the Ce isotopes (4). The values of  $A_J J$  and  $P_{4f}(\text{sat})$  for the RE<sup>3+</sup> ions have been taken from Bleaney (1972) and McCausland and McKenzie (1979)

Isotope	Abundance (%)	Spin $I$	Magnetic moment ( $\mu_N$ )	Quadrupole moment (b)	$A_J J$ (MHz)	$P_{4f}(\text{sat})$ (MHz)
<sup>89</sup> Y	100	$\frac{1}{2}^+$	-0.13742		0	
<sup>141</sup> Pr	100	$\frac{5}{2}^+$	+4.275	-0.059	4372(40)	-2.62(13)
<sup>143</sup> Nd	12.18(6)	$\frac{7}{2}^+$	-1.07	-0.6	-991.4(9)	-5.3(3)
<sup>145</sup> Nd	8.30(6)	$\frac{7}{2}^-$	-0.66	-0.33	-616.0(5)	-2.8(2)
<sup>147</sup> Pm	Radioactive	$\frac{7}{2}^-$	+2.58(7)	+0.74	2396(24)	-6.6
<sup>147</sup> Sm	15.02(2)	$\frac{7}{2}^-$	-0.815	-0.26	-600(8)	-4.8(3)
<sup>149</sup> Sm	13.8(1)	$\frac{7}{2}^-$	-0.672	+0.075	-485(8)	+1.40(7)
<sup>151</sup> Eu	47.8(1.5)	$\frac{5}{2}^+$	+3.472	+0.90	0	0
<sup>153</sup> Eu	52.2(1.5)	$\frac{5}{2}^+$	+1.533	+2.41	0	0
<sup>155</sup> Gd	14.80(5)	$\frac{3}{2}^-$	-2.59	+1.30	42.17	-0.161
<sup>157</sup> Gd	24.86(4)	$\frac{3}{2}^-$	-3.40	+1.36	55.33	-0.172
<sup>159</sup> Tb	100	$\frac{3}{2}^+$	2.014	+1.43	3180(30)	386(20)
<sup>161</sup> Dy	18.9(2)	$\frac{5}{2}^+$	-0.480	+2.51	-821(16)	219(11)
<sup>163</sup> Dy	24.9(2)	$\frac{5}{2}^-$	+0.673	+2.65	1143(22)	228(11)
<sup>165</sup> Ho	100	$\frac{7}{2}^-$	+4.17	+3.49	6497(8)	63(3)
<sup>167</sup> Er	22.95(15)	$\frac{7}{2}^+$	-0.5639	+3.57	-940(9)	-68(3)
<sup>169</sup> Tm	100	$\frac{1}{2}^+$	-0.2316	-1.2	-2333	0
<sup>171</sup> Yb	14.3(2)	$\frac{1}{2}^+$	+0.49367		3105(5)	0
<sup>173</sup> Yb	16.12(21)	$\frac{5}{2}^-$	-0.7989	+2.80	-852(2)	-316(16)
<sup>175</sup> Lu	97.41(2)	$\frac{7}{2}^+$	+2.2327	+3.49	0	0
<sup>176</sup> Lu?	2.59(2)	$\frac{1}{2}^-$	-0.13742			0

$$\begin{aligned}
\mathcal{H}_Q = & \frac{hP_{4f}}{J(2J-1)} \left[ \{3J_z^2 - J(J+1)\} \{I_z^2 - \frac{1}{3}I(I+1)\} \right. \\
& + \frac{1}{2} \{J_z J_+ + J_+ J_z\} \{I_z I_- + I_- I_z\} \\
& + \frac{1}{2} \{J_z J_- + J_- J_z\} \{I_z I_+ + I_+ I_z\} - \frac{1}{4} \{J_+^2 - J_-^2\} \{I_+^2 - I_-^2\} \\
& \left. + \frac{1}{4} \{J_+^2 + J_-^2\} \{I_+^2 + I_-^2\} \right], \quad (5)
\end{aligned}$$

respectively. In the case of the quadrupole interaction we have followed the terminology of McCausland and McKenzie (1979), but with minor variations. An equivalent form, in terms of cubic harmonics, has been given by Abragam and Bleaney (1970).

In RE compounds characterised by large magnetic ordering temperatures  $T_M$ , where  $kT_M \gg A_J \mathbf{I} \cdot \mathbf{J}$ , it is permissible to decouple the electronic and nuclear wavefunctions at temperatures well below  $T_M$ . In this approximation, the magnetic hyperfine interaction takes the form:

$$\mathcal{H}_M = A_J \mathbf{I}_z \langle \mathbf{J}_z \rangle, \quad (6)$$

where it is understood that the precession rate of the 4f electrons greatly exceeds the nuclear Larmor frequency. This approximation can also be used to simplify the quadrupole interaction, which for the hexagonal rare earth metals often takes the form:

$$\mathcal{H}_Q = P_{4f}[I_z^2 - \frac{1}{3}I(I+1)]. \quad (7)$$

Bleaney (1972) has given the values of  $A_J J$  and  $P_{4f}$  (his  $P_{||}$ ) for the fully saturated  $|J_z = J\rangle$  4f shell of the rare earths. For convenience, these too are reproduced in Table 2. But there are occasions, when it is more convenient to have the saturation values of  $A_J J$  and  $P_{4f}$  quoted in terms of the magnetic field (T) and electric field gradient  $V_{zz}$  ( $\text{V m}^{-2}$ ), respectively, at the RE nucleus. For example, the ground state of stable  $^{169}\text{Tm}$  is spin  $\frac{1}{2}$ , which is invisible to nuclear quadrupole interactions. But this is not the case for the excited states of the  $^{169}\text{Tm}$  nucleus. So to facilitate movement between stable and radioactive nuclei, the magnetic fields and the electric field gradients of the fully saturated  $\text{RE}^{3+}$  ions are shown in Table 3.

**Table 3.** Magnetic fields and electric field gradients at the fully saturated  $|J_z = J\rangle$   $\text{RE}^{3+}$  ions, after Stewart (1994) ( $\text{Eu}^{2+}$  is also included)

Ion	Ground state spin $J$	$g_J$	Internal hyperfine field (T)	$V_{zz}(4f)$ ( $10^{21} \text{ V m}^{-2}$ )
$\text{La}^{3+}$	0	0	00	
$\text{Ce}^{3+}$	$\frac{5}{2}$	$\frac{6}{7}$	189.3	22.8
$\text{Pr}^{3+}$	4	$\frac{4}{5}$	335.4	26.2
$\text{Nd}^{3+}$	$\frac{9}{2}$	$\frac{8}{11}$	429.6	11.4
$\text{Pm}^{3+}$	4	$\frac{3}{5}$	419.9	11.7
$\text{Sm}^{3+}$	$\frac{5}{2}$	$\frac{2}{7}$	335.6	-24.5
$\text{Eu}^{3+}$	0	0	0	0
$\text{Eu}^{2+}$	$\frac{7}{2}$	2	-34.2	0
$\text{Gd}^{3+}$	$\frac{7}{2}$	2	-32.1	0
$\text{Tb}^{3+}$	6	$\frac{3}{2}$	311.6	51.1
$\text{Dy}^{3+}$	$\frac{15}{2}$	$\frac{4}{3}$	559.8	55.3
$\text{Ho}^{3+}$	8	$\frac{5}{4}$	724.1	23.8
$\text{Er}^{3+}$	$\frac{15}{2}$	$\frac{6}{5}$	765.3	-25.7
$\text{Tm}^{3+}$	6	$\frac{7}{6}$	662.5	-69.0
$\text{Yb}^{3+}$	$\frac{7}{2}$	$\frac{8}{7}$	412.5	-74.1
$\text{Lu}^{3+}$	0	0	0	0

The relationship between  $P_{4f}$  and  $V_{zz}$  is

$$P_{4f} = \frac{3eQV_{zz}}{h4I(2I-1)}, \quad (8)$$

where  $P_{4f}$  is given in Hz. In the case of the RE vanadates, the ground state will rarely be of the form  $|J_z = J\rangle$ , so it is necessary to calculate  $\langle\psi_G|J_z|\psi_G\rangle$  and  $\langle\psi_G|3J_z^2 - J(J+1)|\psi_G\rangle$  etc., and/or appropriate thermal averages, to arrive at values for  $A\langle J_z\rangle$  and  $P_{4f}$  for the RE ion in question. But if the magnetic ordering temperature  $T_M$  is of the same order of magnitude as the energy splittings caused by the hyperfine interactions, the distinction between electronic and nuclear wavefunctions becomes blurred, and it is necessary to diagonalise both the electronic and nuclear wavefunctions simultaneously. Some examples of mixed electronic and nuclear wavefunctions will be encountered in Section 4c.

Finally, in addition to the intra-ionic contributions to the hyperfine interactions, there will be contributions from the lattice in the form of electric field gradients:

$$\mathcal{H}_Q^{\text{lattice}} = P_{\text{lattice}}[I_z^2 - \frac{1}{3}I(I+1)], \quad (9)$$

where the  $c$ - and  $z$ -axes are taken to be collinear. In general,  $P_{4f}$  and  $P_{\text{lattice}}$  are not simply additive. In addition, it is sometimes necessary to include a pseudo quadrupole interaction, as we shall see below in Section 5a on  $\text{HoVO}_4$ . Finally, there may also be a need to consider Lorentz and demagnetisation fields, internal dipolar fields, core polarisation (particularly for the S state ion Gd) etc. For more complete discussions of these and other terms, the reader is referred to the reviews by Bleaney (1972), McCausland and McKenzie (1979) and Stewart (1994). In general, these terms are usually much smaller than their 4f counterparts, except for  $\text{Gd}^{3+}$  (S-state ion),  $\text{Eu}^{3+}$  ( $J=0$ ), and the non-magnetic ions  $\text{Y}^{3+}$ ,  $\text{La}^{3+}$  and  $\text{Lu}^{3+}$ .

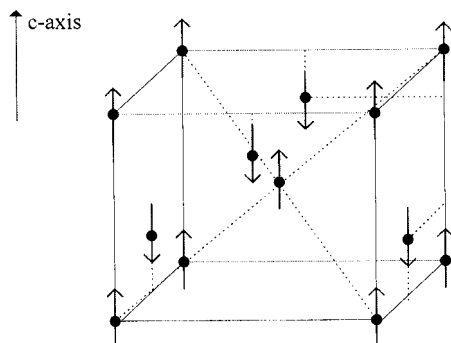


**Fig. 2.** Antiferromagnetic structure in  $\text{YbVO}_4$  below 93 mK. [After Radhakrishna *et al.* (1981).]

#### 4. Antiferromagnetic $\text{YbVO}_4$

Neutron experiments on  $\text{YbVO}_4$  in the mK range by Radhakrishna *et al.* (1981) have shown that  $\text{YbVO}_4$  is an antiferromagnet with a Néel temperature  $T_N$  of some 93 mK. The easy  $c$ -axis antiferromagnetic structure is shown schematically in Fig. 2. Mössbauer experiments have been carried out by Hodges (1983),

who has given a set of crystal field parameters ( $B_{20} = -145, B_{40} = 42.2, B_{60} = -38.3, B_{44} = 870.2, B_{64} = -35.2$  all in  $\text{cm}^{-1}$ ). These parameters can be used to show that the ground state wavefunction is a Kramers doublet:

$$|\psi_g\rangle = \alpha|\pm \frac{7}{2}\rangle + \beta|\mp \frac{1}{2}\rangle, \quad (10)$$

with  $\alpha = 0.912$ . On treating the ground state as a fictitious spin  $\frac{1}{2}$  doublet, it is easy to show that

$$g_{\parallel} = g_J[7\alpha^2 - \beta^2] = 6.46, \quad (11)$$

$$g_{\perp} = g_J4\beta^2 = 0.77, \quad (12)$$

both of which are in reasonable agreement with the EPR results of  $g_{\parallel} = 6.08(1)$  and  $g_{\perp} = 0.85(5)$ , obtained using Yb doped  $\text{YVO}_4$  (Ranon 1968). Thus the  $\text{Yb}^{3+}$  magnetic moments will show little tendency to depart from the  $c$ -axis. In addition, the measured values of the magnetic hyperfine field [324(8) T], the quadrupole interaction ( $V_{zz} = -52.7 \times 10^{21} \text{ V m}^{-2}$ ) (Hodges 1983), and the measured moment of  $3.1(16) \mu_B$  at 50 mK (Radhakrishna *et al.* 1981), are all in reasonable agreement with the ground state assignment of (10).

$$\begin{aligned} E = 354.2 \text{ cm}^{-1} & \text{-----} |\Gamma_6^2\rangle = 0.464|\pm \frac{3}{2}\rangle + 0.886|\mp \frac{5}{2}\rangle \\ E = 288.0 \text{ cm}^{-1} & \text{-----} |\Gamma_7^2\rangle = 0.433|\pm \frac{7}{2}\rangle + 0.901|\mp \frac{1}{2}\rangle \\ \\ E = 63.7 \text{ cm}^{-1} & \text{-----} |\Gamma_6^1\rangle = 0.866|\pm \frac{3}{2}\rangle - 0.464|\mp \frac{5}{2}\rangle \\ E = 0 & \text{-----} |\Gamma_7^1\rangle = 0.901|\pm \frac{7}{2}\rangle - 0.433|\mp \frac{1}{2}\rangle \end{aligned}$$

**Fig. 3.** Energy levels and eigenvectors for the  $\text{Yb}^{3+}$  ion in  $\text{YbVO}_4$ . [After Nipko *et al.* (1997).]

More recently, a new set of crystal field parameters ( $\mathcal{B}_{20} = -215, \mathcal{B}_{40} = 426, \mathcal{B}_{60} = -935, \mathcal{B}_{44} = -706, \mathcal{B}_{64} = 155 \text{ cm}^{-1}$ ), derived from neutron scattering experiments, has been given by Nipko *et al.* (1997). Obviously there is considerable disagreement between the two sets of crystal field parameters. Nevertheless, the eigenvalues and eigenvectors for the first few states of the  $\text{Yb}^{3+}$  ion shown in Fig. 3 are very similar to those of Hodges (1983). Note that the new values of the coefficients  $\alpha$  and  $\beta$ , for the ground state Kramers doublet of (9) differ slightly from those of Hodges (1983), leading to  $g_{\parallel} = 6.28$  and  $g_{\perp} = 0.86$ .

#### (4a) Dipolar Fields in $\text{YbVO}_4$

The primary driving force behind the magnetic ordering in  $\text{YbVO}_4$  is the dipole-dipole interaction between the  $\text{Yb}^{3+}$  magnetic moments, but magnetic exchange may well be present (see Hodges 1983). The contributions to the dipolar field can be obtained by direct summation over a given Lorentz sphere.

**Table 4. Dipolar field matrices**

The matrices were calculated using  $a = 7.0435 \text{ \AA}$  and  $c = 6.247 \text{ \AA}$ , appropriate to  $\text{YbVO}_4$  at  $4.2 \text{ K}$  (Fuess and Kallel 1972). The summation was carried out using a Lorentz sphere of radius  $20 \text{ nm}$ . The symmetry relationships between the various  $\mathbf{D}_{\alpha\beta}$  ( $\alpha, \beta = 1, 4$ ) have been given by Bowden and Clark (1983*b*)

RE site	Dipolar field (T per $\mu_B$ )
Site 1 ( $\mathbf{r} = 0, 0, 0$ )	$D_{11}^{xx} = -2.7658 \times 10^{-3}$ , $D_{11}^{yy} = -2.7658 \times 10^{-3}$ , $D_{11}^{zz} = +5.5314 \times 10^{-3}$
Site 2 ( $\mathbf{r} = 0, a/2, c/4$ )	$D_{21}^{xx} = -4.0221 \times 10^{-2}$ , $D_{21}^{yy} = +5.2630 \times 10^{-2}$ , $D_{21}^{zz} = -1.2408 \times 10^{-2}$
Site 3 ( $\mathbf{r} = a/2, 0, 3c/4$ )	$D_{31}^{xx} = +5.21630 \times 10^{-2}$ , $D_{31}^{yy} = -4.0221 \times 10^{-2}$ , $D_{31}^{zz} = -1.2408 \times 10^{-2}$
Site 4	$D_{41}^{xx} = +2.2549 \times 10^{-3}$ , $D_{41}^{yy} = +2.2549 \times 10^{-3}$ , $D_{41}^{zz} = -4.5098 \times 10^{-3}$

The contributions from the four individual sublattices, taken separately are listed in Table 4. Here  $\mathbf{D}_{11}$  refers to the dipolar field matrix for site 1 arising from unit magnetic moments situated at all site 1 atomic positions,  $\mathbf{D}_{12}$  refers to the dipolar field matrix for site 1 arising from unit magnetic moments from site 2 RE atoms, etc. Thus the total magnetic field at site 1, for example, is given by

$$\mathbf{B}_1 = \mathbf{D}_{11}\boldsymbol{\mu}_1 + \mathbf{D}_{12}\boldsymbol{\mu}_2 + \mathbf{D}_{13}\boldsymbol{\mu}_3 + \mathbf{D}_{14}\boldsymbol{\mu}_4, \quad (13)$$

with similar expressions for  $\mathbf{B}_2$  etc.

Given the results of Table 4, and the ground state of the  $\text{Yb}^{3+}$  ion, it is easy to show that the antiferromagnetic structure shown in Fig. 2 possesses the lowest magnetic energy, in zero applied field. The computed magnetic moment and internal dipolar field are found to be  $3.23 \mu_B$  and  $7.18 \times 10^{-2} \text{ T}$ , respectively, at  $T = 0 \text{ K}$ . The situation is more complicated when a magnetic field is applied along the  $c$ -axis, since it is now necessary to deal with at least two magnetic sub-lattices. Self-consistent calculations, based on dipolar fields only, reveal that the magnetic moment on the spin-down magnetic sublattice should vanish in an applied field of  $6.9 \times 10^{-2} \text{ T}$ . Moreover, because of the large axial magnetic anisotropy, there is little or no tendency for  $\text{YbVO}_4$  to undergo a spin flop. For larger fields, of course, only one sub-lattice needs to be considered, and magnetic saturation can be reached in quite modest applied fields of  $\leq 1 \text{ T}$ . Finally, we remark that results listed in Table 4 can also be used to estimate the dipolar field energies of other spin configurations, including that of  $\text{DyVO}_4$  shown below in Fig. 16.

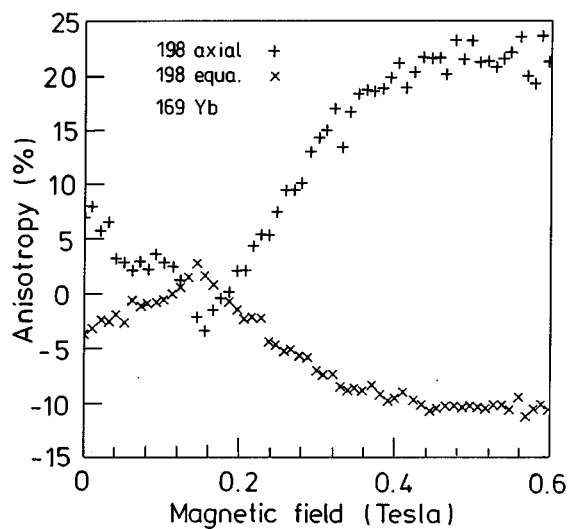


Fig. 4. Axial and equatorial 198 keV  $^{169}\text{Yb}$   $\gamma$ -ray anisotropy as measured in single crystal  $\text{YbVO}_4$ , as a function of magnetic field applied along the  $c$ -axis. [After Hutchison *et al.* (1996).]

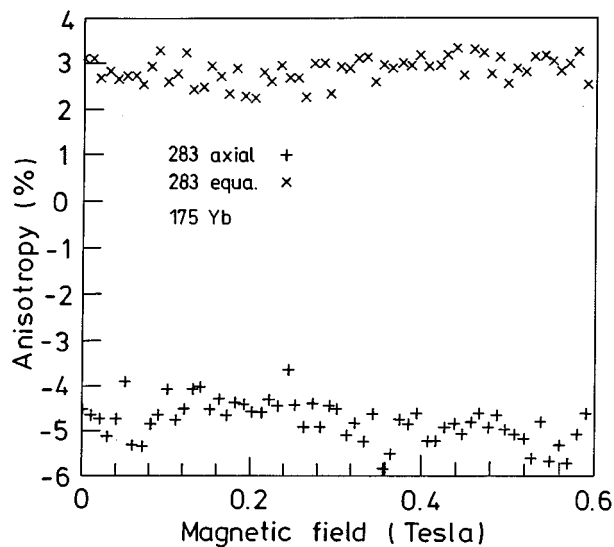


Fig. 5. Axial and equatorial 283 keV  $^{169}\text{Yb}$   $\gamma$ -ray anisotropy as measured in single crystal  $\text{YbVO}_4$ , as a function of magnetic field applied along the  $c$ -axis. [After Hutchison *et al.* (1996).]

#### (4b) $\text{YbVO}_4$ Nuclear Orientation Results

Nuclear orientation studies on  $\text{YbVO}_4$  have been carried out by Hutchison *et al.* (1996), using a  $^3\text{He}/^4\text{He}$  dilution refrigerator to reach temperatures in the mK range. They monitored the 198, 283 and 308 keV and 396 keV  $\gamma$ -rays from

in situ radioactive  $^{169}\text{Yb}$  (half-life 32 d, spin  $I = \frac{7}{2}$ ) and  $^{175}\text{Yb}$  (half-life 4.19 d, spin  $I = \frac{7}{2}$ ), respectively. Some of their results, as a function of magnetic field applied along the  $c$ -axis, can be seen in Figs 4 and 5, for both axial and equatorial detectors.

The results shown in Fig. 4 were analysed using the standard formula for axial geometry:

$$W(\theta) = 1 + B_2 U_2 A_2 P_2(\cos\theta), \quad (14)$$

where the symbols possess their usual meanings (e.g. Stone and Postma 1986). For the  $^{169}\text{Yb}$  198 keV  $\gamma$ -ray, the value of  $A_2 U_2$  was set equal to  $0.6550 \times 8214$  (Davva *et al.* 1987; Benoit *et al.* 1972), and the thermal orientation parameter  $B_2$  was calculated using a temperature of 44(2) mK, estimated by warming the sample in the presence of a  $^{60}\text{Co}$  thermometer, and noting the temperature at which the  $^{169}\text{Yb}$   $\gamma$ -ray anisotropy began to change. The values of the hyperfine parameters  $a$  and  $P$ , defined by

$$\mathcal{H} = aI_z + P[I_z^2 - \frac{1}{3}I(I+1)], \quad (15)$$

were estimated to be  $a = 460(17)$  MHz and  $P = -112.5(6.5)$  MHz (1 mK = 20.8 MHz) for the  $^{169}\text{Yb}$  nucleus, based on the Mössbauer results of Hodges (1983), and tabulated magnetic and quadrupole moments (CRC Handbook of Spectroscopy 1981). Thus the expected NMRON  $^{169}\text{Yb}$  resonance, for the lowest transition, should be at 1.13(5) GHz (53 mK).

Given the relative magnitudes of  $a$  and  $P$ , it is evident that the quadrupole interaction will dominate. For example, above the Néel temperature of 93 mK, the nuclear ground state of  $^{169}\text{Yb}$  should be  $|I_z = \pm \frac{7}{2}\rangle$  with the first excited state  $|I_z = \pm \frac{5}{2}\rangle$  some 670 MHz (33mK) higher in energy. Thus even above  $T_N$ , there should be appreciable nuclear alignment. However, experimentally, little or no NO 198 keV signal was found at temperatures just above 100 mK. Moreover, at lower temperatures, comparison between theory and experiment for the  $^{169}\text{Yb}$  results quickly showed that the measured 198 keV  $\gamma$ -ray anisotropy was again much lower than expected, except perhaps in high applied fields. Note that in an applied field of 0.15 T, the axial anisotropy reaches a sharp minimum of 4%. It is tempting to ascribe this minimum to the demagnetisation of the spin-down sublattice, as  $B$  is increased. However, as we shall see below, caution is required in the interpretation of the 198 keV  $\gamma$ -ray NO results.

By way of contrast, the  $^{175}\text{Yb}$  (283 keV)  $\gamma$ -ray anisotropy shows almost no variation over the entire magnetic field range. Since the latter possesses a spin of  $\frac{7}{2}^-$ , a magnetic moment  $\mu = 0.6 \mu_N$ , and an estimated  $Q$  of 2 b (A. Stuchbury, personal communication), compared with  $I = \frac{7}{2}^+$ ,  $0.63 \mu_N$  and  $Q = +2.80$  b for  $^{169}\text{Yb}$  (CRC Handbook of Spectroscopy 1981), the hyperfine splittings of these two isotopes should be similar. So similar NO behaviour, in applied magnetic fields, might be anticipated.

These difficulties have been resolved by Hutchison *et al.* (1996) who have ascribed the low 198 keV  $\gamma$ -ray anisotropy in the  $^{169}\text{Yb}$  results to intermediate state reorientation in the 316 keV  $^{169}\text{Tm}$  level. The 198 keV  $\gamma$ -ray is fed from the 316 keV  $^{169}\text{Tm}$   $\frac{7}{2}^+$  level which has a lifetime of 660 ns. Since the

nuclear hyperfine time-scale is  $\tau_{\text{hyp}} \ll 660$  ns, intermediate state reorientation can take place in this level. Further, all  $\gamma$ -rays emanating from this particular level, show anomalous behaviour, whereas others, such as the 283 keV  $^{175}\text{Yb}$  shown in Fig. 5 do not. Nevertheless, despite the strong evidence for intermediate state reorientation, no mechanism was identified. This problem is re-examined in the next section, where a novel mechanism for intermediate state reorientation is presented and discussed.

(4c) *Intermediate Reorientation in Antiferromagnetic YbVO<sub>4</sub>*

A review of intermediate reorientation has been given by Krane (1986). One of the key equations is the time evolution of the nuclear density matrix:

$$\rho(t) = e^{-i\mathcal{H}_n t/\hbar} \rho(0) e^{i\mathcal{H}_n t/\hbar}, \quad (16)$$

where (i) the initial density matrix  $\rho(0)$  is determined by the polarisation of the parent radioactive isotope and (ii) the Hamiltonian  $\mathcal{H}_n$  is that appropriate to the nuclear level in which intermediate state reorientation is taking place. Of course, it is also necessary to include lifetime effects, but equation (16) is at the heart of the matter.

At first sight it is very difficult to see any mechanism that can give rise to intermediate state reorientation in YbVO<sub>4</sub>. Given that the initial density matrix  $\rho(0)$  and the Hamiltonian  $\mathcal{H}_n$  are both of axial form, no change in  $\rho(t)$  should occur, because the commutator  $[\rho(0), \mathcal{H}_n] = 0$ . For intermediate state reorientation to take place, off-diagonal terms in the Hamiltonian are mandatory.

In the past, several mechanisms for intermediate state reorientation have been identified: (i) one off-diagonal terms in the magnetic hyperfine interaction  $A_J \mathbf{I} \cdot \mathbf{J}$ , (ii) one off-diagonal terms induced by small applied and/or internal magnetic fields, at right angles to the principal axis of quantisation, and (iii) one and two off-diagonal terms in the lattice quadrupolar interaction (Strohm and Sapp 1963; Daniels and Misra 1966; Wäppling *et al.* 1973; Haroutunian *et al.* 1980). The latter two mechanisms are clearly inoperative. YbVO<sub>4</sub> is tetragonal, with a strong *c*-axis direction of easy magnetisation. Thus the perturbing Hamiltonian would appear to take the diagonal form of (15). Moreover, any effects due to the off-diagonal terms in the magnetic hyperfine interaction  $A_J \mathbf{I} \cdot \mathbf{J}$  will be much reduced because of the small  $g_{\perp}$  factor in the *a*-*a'* plane. Calculation reveals that, in zero applied field, such terms can give rise to a small pseudo-quadrupole interaction  $\sim 1$  MHz, at temperatures  $\sim 50$  mK.

However, it is important to realise that the electronic state of the 316 keV level in question is Tm<sup>3+</sup> ( $J = 6$ ), not Yb<sup>3+</sup> ( $J = \frac{7}{2}$ ). Thus a knowledge of the electronic Tm<sup>3+</sup> electronic levels is required. These can be found, either by using the set of crystal field parameters given say by Hodges (1983) for YbVO<sub>4</sub>, and subsequently adapting them to TmVO<sub>4</sub>, or alternatively by using the set of energy levels for TmVO<sub>4</sub> given in Section 15 below. Both procedures give similar ground and first excited state wavefunctions. Using the results shown in Fig. 17, the Tm<sup>3+</sup> ground state wavefunction is a non-Kramers doublet:

$$|\psi_g\rangle = \alpha|\pm 5\rangle + \beta|\pm 1\rangle + \gamma|\mp 3\rangle, \quad (17)$$

where  $\alpha = 0.92$ ,  $\beta = -0.37$  and  $\gamma = 0.12$ , with the first excited state lying at  $54 \text{ cm}^{-1}$ . The calculated  $g$ -values are  $g_{\parallel} = 11.78$  and  $g_{\perp} = 0$ .

To make further progress, it is necessary to make some assumptions. In the first place we shall assume that following electron capture by the  $^{169}\text{Yb}$  nucleus, the resulting  $\text{Tm}^{3+}$  electronic configuration rapidly takes up that of the ground state of equation (17). If this assumption is correct then it is easy to see that the one off-diagonal terms in the magnetic hyperfine interaction  $A_J \mathbf{I} \cdot \mathbf{J}$  cannot lift the degeneracy of the  $\text{Tm}^{3+}$  doublet. But this is not the case for the intra-ionic quadrupole hyperfine interaction of equation (5). Neglecting for the moment any applied magnetic fields, the nuclear quadrupole interaction can be written in the block diagonal  $2 \times 2$  form:

$$\mathcal{H}_Q = \begin{array}{cc} \begin{array}{c} |\psi_g\rangle \\ P[I_z^2 - I(I+1)/3] + \frac{1}{2}A_{\parallel}I_z \end{array} & \begin{array}{c} |\psi_g'\rangle \\ P'I_+^2 + P''I_-^2 \end{array} \\ \begin{array}{c} P''I_+^2 + P'I_-^2 \end{array} & \begin{array}{c} P[I_z^2 - I(I+1)/3] - \frac{1}{2}A_{\parallel}I_z \end{array} \end{array} \quad (18)$$

where (i)

$$A_{\parallel}(\text{Tm}) = A_J(\text{Tm})(g_{\parallel}/g_J), \quad (19)$$

(ii)

$$P = \frac{hP_{4f}(\text{Tm})}{66} [24(3\alpha^2 + \gamma^2) - 39], \quad (20)$$

(iii)

$$P' = \frac{hP_{4f}(\text{Tm})}{66} [2\alpha\gamma\sqrt{11 \times 15} + 21\beta^2], \quad (21)$$

and (iv)

$$P'' = \frac{hP_{4f}(\text{Tm})}{66} [12\beta\gamma]. \quad (22)$$

Using the ground state  $\text{Tm}^{3+}$  wavefunction of (17), we estimate (i)  $P_{4f}(\text{Tm}) \sim 40 \text{ MHz}$ , and (ii)  $P'/P = 0.256$  and  $P''/P = 0.024$ . To these terms, of course, we should add the diagonal lattice contribution. Note that for the  $316 \text{ keV } ^{169}\text{Tm}$  ( $I = \frac{7}{2}$ ) level,  $\mathcal{H}_Q$  is a  $16 \times 16$  matrix.

Given the degeneracy associated with the diagonal terms of (18), it is immediately obvious that admixing of the nuclear Zeeman levels will take place, at a rate determined primarily by the strength of the off-diagonal terms. Since  $P'$  is  $\sim 10 \text{ MHz}$ , the characteristic time associated with admixing of the Zeeman wavefunctions should be  $100 \text{ ns}$ . Thus the lifetime ( $660 \text{ ns}$ ) of the  $316 \text{ keV}$  level is long enough for significant reorientation to take place. This, in turn, will reduce the value of the thermal orientation parameter  $B_2$ , resulting in a lower  $^{169}\text{Yb}$   $198 \text{ keV}$

$\gamma$ -ray anisotropy. Finally, we note that intermediate state reorientation in the original  $\text{Yb}^{3+}$  state, by the quadrupolar mechanism, cannot take place because the off-diagonal matrix elements of the form  $\langle \alpha(\frac{7}{2}) | + \beta \langle -\frac{1}{2} | | \mathcal{H}_Q | | \alpha(-\frac{7}{2}) \rangle + \beta | \frac{1}{2} \rangle \rangle$  are identically zero.

Below  $T_N$ , the situation is much more complicated. In the first place, it is necessary to include internal/applied magnetic fields, and take into account two dissimilar sublattices. In the ferromagnetic regime however, the Hamiltonian takes the form:

$$\begin{array}{cc}
 |\psi_g\rangle & |\psi_g'\rangle \\
 +\frac{1}{2}g_{||}\mu_B B \mathbf{E} - g_N \mu_{BN} I_z B & \\
 +P[I_z^2 - I(I+1)/3] + \frac{1}{2}A_{||}I_z & P'_+ I_+^2 + P'' I_-^2 \\
 \mathcal{H}_N = & (23) \\
 & -\frac{1}{2}g_{||}\mu_B B \mathbf{E} - g_N \mu_{BN} I_z B \\
 P' I_+^2 + P'' I_-^2 & +P[I_z^2 - I(I+1)/3] - \frac{1}{2}A_{||}I_z
 \end{array}$$

where  $\mathbf{E}$  is the unit  $8 \times 8$  matrix for  $I = \frac{7}{2}$  nuclei. Nevertheless, despite the complexity of equation (23), one simple observation can be made. In the presence of large magnetic fields, the splitting of the fictitious spin  $\frac{1}{2}$  electronic doublet is increased, which has the effect of reducing admixing caused by the off-diagonal quadrupole terms. In essence therefore, we have a 'tuneable' intermediate state reorientation. In large magnetic fields, the  $\gamma$ -ray anisotropy should increase, as observed experimentally.

Finally, it should be acknowledged that the above discussion is qualitative rather than quantitative. But the reader is warned that the real situation is very complicated. Some difficulties are: (i) the  $\text{Tm}^{3+}$  electronic state taken up, following electron capture, is open to debate, (ii) a knowledge of the behaviour of both sublattices in an applied field is required, (iii) the quadrupole moment  $Q$  of the 316 keV  $^{169}\text{Tm}$  level is not known with precision, and (iv) perhaps more importantly, the  $^{169}\text{Tm}$  316 keV (660 ns) level is also preceded by a  $^{169}\text{Tm}$  379 keV (50 ns) level. So that in practice, two successive reorientation processes need to be considered.

#### (4d) NMR Enhancement in $\text{YbVO}_4$

Despite much effort by the ADFA Low Temperature Group, no  $^{169}\text{Yb}$  NMR resonances have been identified. One possible culprit could be a low NMR enhancement factor  $\eta$ . Since the transition probability for exciting resonances is proportional to  $(1+\eta)^2$ , a large NMR enhancement constitutes a considerable advantage. Moreover, if  $\eta$  is small it will be difficult to resonate the nuclear spins without unduly heating the cold copper finger to which they are attached. Each NMR enhancement factor is specific to the vanadate in question.

To estimate the NMR enhancement factor in  $\text{YbVO}_4$  we make the following assumptions. At low temperatures, only the ground state doublet of (10) is important, which is split by the presence of a dipolar magnetic field  $B_z$ . Thus

the magnetic moment of a single  $\text{Yb}^{3+}$  ion at temperature  $T$  is given by

$$M_z = \frac{1}{2}g_z\mu_B \tanh(\Delta/2kT), \quad (24)$$

where the doublet splitting is given by

$$\Delta = g_z\mu_B B_z \quad (25)$$

and  $g_z(=g_{||})$  is given by (11). If a small field  $B_x$  is applied along the  $x$ -axis, the magnetic moment will tip slightly in that direction. The amount of tip is determined by the susceptibility:

$$\chi_{xx} = 2 \frac{(g_z\mu_B)^2}{\Delta} \tanh(\Delta/2kT) 4\beta^2 = \frac{(g_x\mu_B)^2}{2\Delta} \tanh(\Delta/2kT), \quad (26)$$

where  $g_x(=g_{\perp})$  is given by (12).

We are now in a position to work out the tip-angle  $\theta$  through which the spins are tipped by the application of a small (RF field)  $B_x$ . We find

$$\tan\theta \approx \theta = \frac{M_x}{M_z} = \left[ \frac{g_x}{g_z} \right]^2 \frac{B_x}{B_z}. \quad (27)$$

Moreover, because the magnetic hyperfine field is tipped through the same angle  $\theta$ , the transverse hyperfine field  $(B_{\text{hpf}})_x$  is given by

$$(B_{\text{hpf}})_x = B_{\text{hpf}} \left[ \frac{g_x}{g_z} \right]^2 \frac{B_x}{B_z}. \quad (28)$$

Thus the NMR enhancement factor is given by

$$\eta = \frac{(B_{\text{hpf}})_x}{B_x} = \left[ \frac{g_x}{g_z} \right]^2 \frac{B_{\text{hpf}}}{B_z}. \quad (29)$$

If we use (i)  $g_z = 6.46$ ,  $g_x = 0.77$ , (ii)  $B_{\text{hpf}} = 324$  T, and (iii)  $B_z = 0.1$  T, we find that the NMR enhancement factor  $\eta$  is  $\sim 46$ . But for  $B_z = 0.6$  T, it falls to  $\sim 7.7$ . We conclude therefore that in zero applied field the NMR enhancement factor is healthy, but it can be reduced to much smaller values by the application of quite modest applied fields. In the next section we shall see how this effect can be put to good use in the thermometric detection of NMR in stable isotopes.

#### (4e) Thermometric Detection of NMR in Antiferromagnetic $\text{YbVO}_4$

NMR in the mK regime can be detected simply by monitoring the heat deposited in the  $^3\text{He}/^4\text{He}$  dilution refrigerator, following resonant absorption. In such thermometric experiments, it is necessary to use a stable isotope with a

reasonable percentage abundance, so that the energy absorbed from the RF field by the nuclei is significant. The temperature of the refrigerator can be monitored using a  $^{60}\text{Co}/\text{Co}$  thermometer, which at temperatures of  $\sim 10$  mK is sensitive to heating at the  $\mu\text{W}$  level.

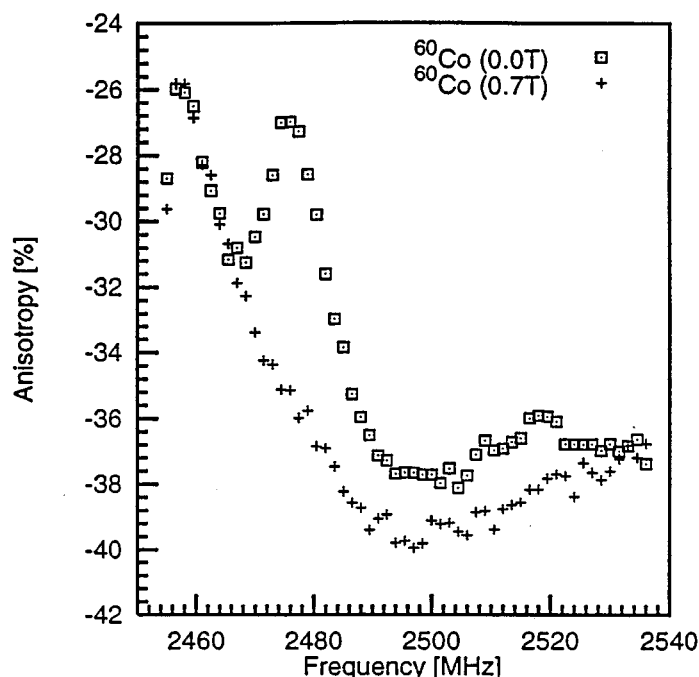


**Fig. 6.** Thermometric NMR resonance of the stable isotope  $^{171}\text{Yb}$  spin nucleus in  $\text{YbVO}_4$  at 2475(5) MHz. [After Prandolini *et al.* (1997).]

In Fig. 6 the thermometric resonance of the 14.3% abundant  $^{171}\text{Yb}$  ( $I = \frac{1}{2}$ ) resonance can be seen at 2475(5) MHz (Prandolini *et al.* 1997). This frequency corresponds to a magnetic hyperfine field of 328.8(6) T, in very reasonable agreement with the value of 324(8) T obtained by Hodges (1983) from  $^{170}\text{Yb}$  Mössbauer measurements. In this experiment the temperature of the crystal was estimated to be at 45 mK, with the cold copper finger at 9 mK.

In such experiments, it is mandatory to guard against RF cable and/or coil resonances, which can simulate resonant behaviour. Such non-NMR resonances can be identified in separate experiments with the sample removed. Alternatively, magnetic fields can be applied, to reduce the NMR enhancement factor, and/or shift the NMR resonance. The results of such an experiment are also shown in Fig. 6. It will be observed that the resonance at 2475(5) MHz is suppressed by an applied field of 0.7 T, in accord with our remarks made in the Section 4*d*.

It is also worth observing that the linewidth of the 2475(5) MHz resonance is predominantly homogeneous (14 MHz), as a result of spin-spin interactions between the concentrated  $^{171}\text{Yb}$  nuclei. This is in marked contrast to NMRON experiments in antiferromagnets with dilute radioactive impurities, where narrow linewidths ( $\sim 50$  kHz) are frequently encountered. Thus in practice, NMR

resonance searches using stable nuclei in antiferromagnets are easier to perform, because the frequency range in question can be covered using coarser steps.

Finally, we also remark that the  $^{171}\text{Yb}$  resonance shown in Fig. 6 has been observed, simultaneously, using an internal radioactive  $^{175}\text{Yb}$  thermometer (Prandolini *et al.* 1997).

(4f) *Self-cooling in YbVO<sub>4</sub>*

The antiferromagnet phosphate  $\text{DyPO}_4$  has many similarities with  $\text{YbVO}_4$ . The former is characterised by a Néel temperature of 3.390 K and a very large *c*-axis anisotropy (Wright *et al.* 1971; Koonce *et al.* 1971). Moreover for fields applied along the easy *c*-axis, it undergoes a sharp first order AF-PM transition (a metamagnetic transition) at 0.545(1) T for temperatures below 0.75 K. This suggests that this compound could be used as a magnetic refrigerant. It is also possible that similar behaviour might occur in  $\text{YbVO}_4$ .

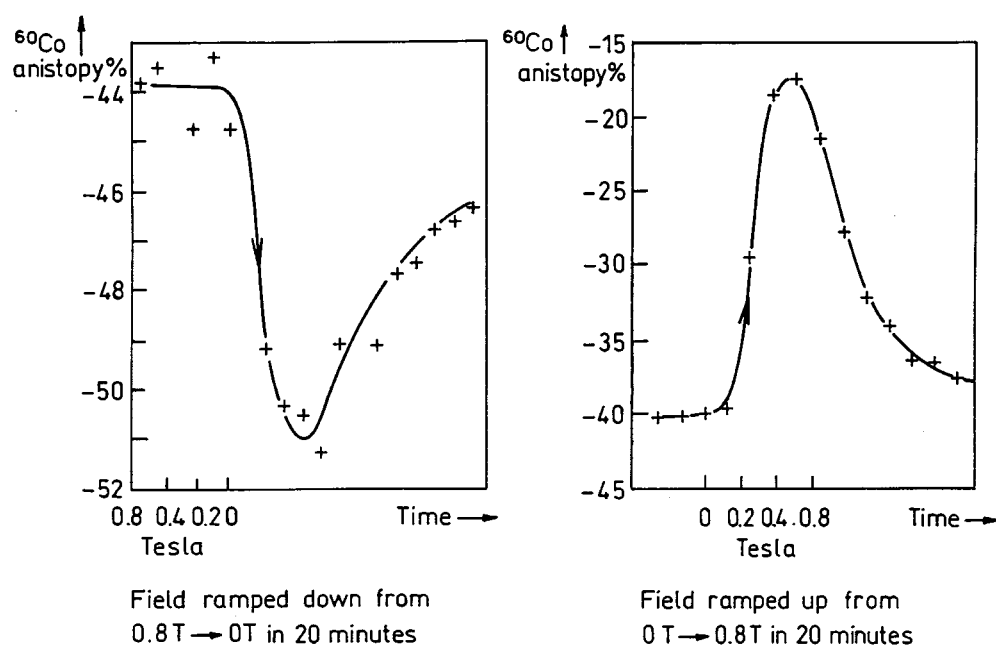
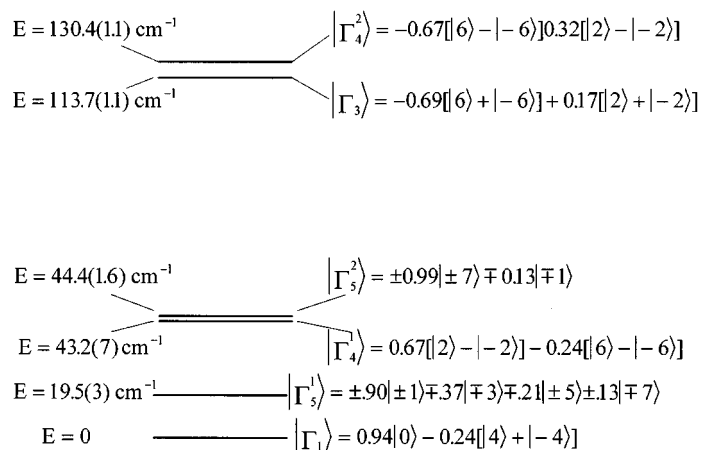


Fig. 7. Self-cooling/heating in single crystal  $\text{YbVO}_4$  induced by magnetic fields applied along the *c*-axis. [After Hutchison *et al.* (1997).]

Some preliminary self-cooling/heating experiments have been performed using  $\text{YbVO}_4$ . The temperature of the cold copper finger, plus crystal, was monitored using a  $^{60}\text{Co}$  thermometer. The results can be seen in Fig. 7, where it will be observed that the  $^{60}\text{Co}$  record shows a marked cooling of the refrigerator, as the magnetic field is removed, followed by heating when the field is re-applied. In both these experiments, the magnetic field was ramped up or down in 20 minutes. So there is a considerable time delay, between the cooling and/or heating of the  $^{60}\text{Co}$  thermometer, due to the presence of the Kapitza boundary between the  $\text{YbVO}_4$  crystal and the cold copper finger. As expected experiments performed

with longer ramp up/down times (500 minutes) show reduced changes in the  $^{60}\text{Co}$  record, but they do allow a clear minimum/maximum to be observed between 0.1–0.2 T. Clearly more work is required to fully quantify this effect, but it is clear that  $\text{YbVO}_4$  could be used as a magnetic refrigerator, in a rather novel manner.



**Fig. 8.** Energy levels and eigenvectors for the  $\text{Ho}^{3+}$  ion in  $\text{HoVO}_4$ . [After Skanthakumar *et al.* (1995).] Only the first six energy levels are shown. The next energy level is at  $226(4) \text{ cm}^{-1}$ .

## 5. The van Vleck Paramagnet $\text{HoVO}_4$

Recently, the crystal field levels of the  $\text{Ho}^{3+}$  ion in  $\text{HoVO}_4$  have been determined by neutron scattering techniques by Skanthakumar *et al.* (1995), who gave an optimised set of crystal field parameters ( $\mathcal{B}_{20} = -164$ ,  $\mathcal{B}_{40} = 302$ ,  $\mathcal{B}_{60} = -740$ ,  $\mathcal{B}_{44} = -890$ ,  $\mathcal{B}_{64} = 114 \text{ cm}^{-1}$ ). The low lying energy levels of the  $\text{Ho}^{3+}$  ion are summarised in Fig. 8. A rival set of energy levels and crystal field parameters ( $B_{20} = -96.20$ ,  $B_{40} = 42.97$ ,  $B_{60} = -45.79$ ,  $B_{44} = -8361$ ,  $B_{64} = 83.41 \text{ cm}^{-1}$ ), in accord with the definition of equation (1), has also been given by Bleaney *et al.* (1988). In general, there is good agreement concerning the energy levels and eigenvectors, particularly for the low lying energy states.

Of particular interest is the first excited state doublet  $\Gamma_5^1$  at  $19.5(3) \text{ cm}^{-1}$ . Using laser spectroscopy, Battison *et al.* (1975, 1977) have shown that this doublet, which they place at  $21 \text{ cm}^{-1}$  is split with a separation of  $2.0 \text{ cm}^{-1}$  ( $\sim 60 \text{ GHz}$ ) below 20 K. This splitting might be due to a weak distortion of the tetragonal structure. However, a careful neutron study by Kazei and Popov (1994) has shown that  $[a/b-1]$  is less than  $4 \times 10^{-5}$ . Thus the origin of the splitting of the first excited state is still obscure.

From an examination of Fig. 8, it will be observed that the non-magnetic singlet ground state is predominantly  $|J_z = 0\rangle$ , while the excited state is predominantly  $|J_z = \pm 1\rangle$ . For many purposes therefore, the ground state may be represented by a non-magnetic singlet  $|J_z = 0\rangle$ , with an excited state doublet  $|J_z = \pm 1\rangle$  some  $21 \text{ cm}^{-1}$  higher. Thus  $\text{HoVO}_4$  is an archetypal van Vleck paramagnet, exhibiting a temperature independent susceptibility, for magnetic fields applied

in the  $a$ - $b$  plane, below say 10 K. To see how this comes about, consider the response of the ground state energy to a magnetic field applied say along the  $a$ -axis of the  $\text{HoVO}_4$  crystal. The appropriate perturbation to the crystal field Hamiltonian  $\mathcal{H}_{\text{CF}}$  is given by

$$\mathcal{H}' = g_J \mu_B J_x B. \quad (30)$$

Thus the first order correction to the ground state energy is zero, whereas the second order contribution is given by

$$E'' = \sum_{\pm 1} \frac{|\langle J_z = 0 | \mathcal{H}' | J_z = \pm 1 \rangle|^2}{\Delta} = -\frac{1}{2} \chi_{\text{vv}} B_x^2, \quad (31)$$

with the temperature independent van Vleck susceptibility

$$\chi_{\text{vv}} = \frac{18(g_J \mu_B)^2}{\Delta}. \quad (32)$$

An identical expression is also obtained for fields applied along the  $y$ -axis. Experimentally  $\chi_{\text{vv}}$  is found to be  $2.32 \mu_B/\text{T}$  (Bleaney *et al.* 1976, 1978). Note that the magnetic moment is

$$M_x = -\frac{\partial E}{\partial B_x} = \chi_{\text{vv}} B_x, \quad (33)$$

i.e. linear in the applied field within the  $a$ - $a'$  plane. Of course, in larger fields magnetic saturation will occur. Details of the magnetic properties of  $\text{HoVO}_4$  in strong magnetic fields have been given by Andronenko *et al.* (1985).

#### (5a) Enhanced Nuclear Magnetism in $\text{HoVO}_4$

A review of enhanced nuclear magnetism, and applications, has been given by Abragam and Bleaney (1983).  $\text{HoVO}_4$  is a classic example of an enhanced nuclear system, with a Néel temperature 4.8 mK. In this section, the basic properties of enhanced nuclear magnetism are reviewed.

In the presence of the magnetic hyperfine interaction  $A_J \mathbf{I} \cdot \mathbf{J}$ , the bare nuclear moment, in the  $x$ - $y$  plane, is enhanced by a 4f electronic component. The nuclear moment, say  $\mu_x (= g_N \mu_N I_x)$ , can be envisaged as generating a magnetic field  $B_A$  which acts on the 4f electrons:

$$A_J I_x J_x \equiv g_J \mu_B J_x B_A, \quad (34)$$

where

$$B_A = \frac{A_J}{g_J \mu_B} I_x. \quad (35)$$

Thus, by virtue of (33), there will be an induced van Vleck magnetic moment on the 4f shell:

$$M_x = \chi_{\text{vv}} B_A = \left( \frac{\chi_{\text{vv}} A_J}{g_J \mu_B} \right) I_x = K_x g_N \mu_N I_x, \quad (36)$$

where the enhancement factor  $K_x$ , relative to the bare nuclear magnetic moment, is given by

$$K_x = \frac{\chi_{\text{vv}} A_J}{(g_J \mu_B)(g_N \mu_N)}. \quad (37)$$

An identical value is found for  $K_y$ , but  $K_z \sim 0$ . Following NMR experiments carried out in the paramagnetic range,  $K_x$  was found to be  $\sim 170$  (Bleaney *et al.* 1978). Thus in the presence of an applied field, the Zeeman interaction takes the form

$$\mathcal{H}_z = g_N \mu_N (1 + K) \mathbf{I} \cdot \mathbf{B}, \quad (38)$$

where  $K$  is 170 for fields applied in the  $x$ - $y$  plane and zero otherwise.

To the Zeeman hyperfine interaction, we must also add the quadrupole terms. There are three contributions: from the lattice  $P_{\text{latt}}$ , from the intra-ionic 4f shell  $P_{4f}$ , and from the pseudo-quadrupole interaction  $P_{\text{PQ}}$ . The latter is generated by the nuclear hyperfine interaction  $A_J \mathbf{I} \cdot \mathbf{J}$ , which causes admixing between the ground and first excited states. On using second order perturbation theory we find

$$\mathcal{H}_Q^{\text{PQ}} = \sum_{\pm 1} \frac{|\langle J_z = 0 | A_J \mathbf{I} \cdot \mathbf{J} | J_z = \pm 1 \rangle|^2}{E_G - E_{\pm 1}} = P_{\text{PQ}} [I_z^2 - \frac{1}{3} I(I+1)]. \quad (39)$$

From experiment, it is found that  $\gamma_{\perp}/2\pi = 1526(3)$  MHz/T, and  $P = 25.9(2)$  MHz. For a discussion of the breakdown of the measured quadrupole parameter  $P$  into its three components, the reader is referred to Bleaney *et al.* (1978).

In practice, the enhanced nuclear magnetic moment in  $\text{HoVO}_4$  is about  $0.4 \mu_B$  per Ho site. Thus  $\text{HoVO}_4$  will enter an ordered state, in the mK as opposed to the  $\mu\text{K}$  range (Bleaney 1980). The challenge therefore is to determine the magnetic structure of the ordered state, in both zero and small applied magnetic fields.

#### (5b) Magnetic Structure Determination in $\text{HoVO}_4$

Initially, the ordered magnetic structure of  $\text{HoVO}_4$  was determined by adiabatic self-cooling experiments to 1 mK, followed by NO studies using in situ radioactive  $^{166\text{m}}\text{Ho}$ . This work led to the development of ‘average statistical tensor plots’, which could be used to determine (i) the temperature reached and (ii) spin configurations in small applied fields. The principle is illustrated, schematically, in Fig. 9.

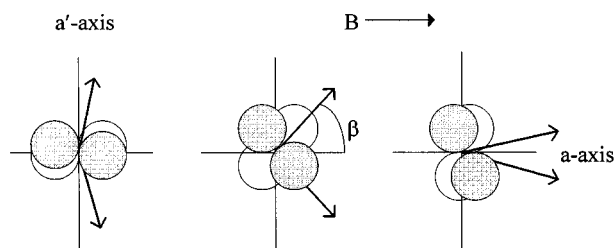


**Fig. 9.** A 2D schematic representation of dipolar emission from a two sub-lattice antiferromagnet, in an ever increasing magnetic field. Note that when the spins are at right angles to each other (middle drawing) the  $\gamma$ -ray emission along the  $a$  and  $a'$  axes will be identical.

Clearly a detector placed say along the  $a'$ -axis will see marked changes as the spins are rotated towards the  $a$ -axis. The key references to this work are Bowden *et al.* (1979), Allsop *et al.* (1979, 1980, 1981, 1984*a*, 1984*b*) and Clark *et al.* (1987). A review of work prior to 1986, and related methods, has been given by Turrell (1986).

In  $\text{HoVO}_4$ , the situation is a little more complex than that depicted in Fig. 9. In the first case the appropriate Hamiltonian is non-axial, because the enhanced nuclear spins are forced to lie in the  $a$ - $a'$  plane. So it is advantageous to change to a new set of axes where the new  $z$ -axis is collinear with the enhanced nuclear magnetic moment. In the new frame of reference we have

$$\mathcal{H} = -g_N(1 + K)\mu_N B_z + P\left\{-\frac{1}{2}[I_z^2 - \frac{1}{3}I(I + 1)] + \frac{1}{4}(I_+^2 + I_-^2)\right\}. \quad (40)$$

[Note the factor of  $\frac{1}{4}$  in equation (40). This corrects a misprint in Bowden *et al.* (1979) and Turrell (1986). However, the tables produced by Bowden *et al.* (1979) were calculated with the factor  $\frac{1}{4}$ .]

Thus the simple axial  $\gamma$ -ray emission formula of (14) is no longer valid and we write

$$\begin{aligned} W(\theta, \varphi) - 1 = & \sqrt{2I_1 + 1}\{A_2(\gamma)[\rho_0^2 \frac{1}{2}(3\cos^2\theta - 1) + \rho_2^2 \sqrt{\frac{3}{2}}(1 - \cos^2\theta)\cos 2\varphi] \\ & + A_4(\gamma)[\rho_0^4 \frac{1}{8}(35\cos^4\theta - 30\cos^2\theta + 3) + \rho_2^4 \frac{1}{2} \sqrt{\frac{5}{2}}(1 - \cos^2\theta)(7\cos^2\theta - 1)\cos 2\varphi] \\ & + \rho_4^4 \frac{1}{4} \sqrt{\frac{35}{2}}(1 - \cos^2\theta)^2 \cos 4\varphi\}, \end{aligned} \quad (41)$$

where (i) it is understood that the  $\gamma$ -ray emission, in the direction  $(\theta, \varphi)$ , is with respect to the local magnetic axes (not laboratory axes) of the spin in question, (ii) the  $\rho_Q^K$  are statistical tensors (thermal parameters), (iii) the  $A_{2,4}(\gamma)$  are nuclear parameters, and (iv) only the even terms ( $n = 0, 2$  and  $4$ ) are required for NO experiments where the  $\gamma$ -ray polarisation is not recorded. For  $^{166\text{m}}\text{Ho}$ ,  $A_2(\gamma) = 0.273$ ,  $A_4(\gamma) = 0.0$  for the 712 keV transition, while  $A_2(\gamma) = 0.075$ ,  $A_4(\gamma) = 0.431$  for the 810 keV transition. Thus the 810 keV transition allows information to be gleaned from both second and fourth rank statistical tensors.

Equation (41) is that appropriate to a single spin pointing along say the  $a$ -axis. For two spins, it is necessary to define a set of average statistical tensors

$\bar{\rho}_Q^K$  with respect to the laboratory axes. Since the statistical tensors obey well known rotational properties, it is easy to show that (41) still holds, but with the local statistical tensors  $\rho_Q^K$  replaced by their average counterparts:

$$\begin{aligned}\bar{\rho}_0^2 &= \rho_0^2(3\cos^2\beta - 1) - \sqrt{\frac{3}{2}}\rho_2^2\sin^2\beta, \\ \bar{\rho}_2^2 &= \rho_0^2\frac{1}{2}\sqrt{\frac{3}{2}}\sin^2\beta + \rho_2^2(1 - \frac{1}{2}\sin^2\beta), \\ \bar{\rho}_0^4 &= \rho_0^4\frac{1}{8}(35\cos^4\beta - 30\cos^2\beta + 3) - \rho_2^4\frac{1}{2}\sqrt{\frac{5}{2}}(1 - \cos^2\beta)(7\cos^2\beta - 1) \\ &\quad + \rho_0^4\frac{1}{4}\sqrt{\frac{35}{2}}\sin^4\beta, \\ \bar{\rho}_2^4 &= -\rho_0^4\frac{1}{4}\sqrt{\frac{5}{2}}(1 - \cos^2\beta)(7\cos^2\beta - 1) + \rho_2^4\frac{1}{2}(7\cos^4\beta - 6\cos^2\beta + 1), \\ \bar{\rho}_4^4 &= \rho_0^4\frac{1}{8}\sqrt{\frac{35}{2}}\sin^4\beta - \rho_2^4\frac{\sqrt{7}}{4}\sin^2\beta(1 + \cos^2\beta) + \rho_4^4\frac{1}{8}(1 + 6\cos^2\beta + \cos^4\beta),\end{aligned}\quad (42)$$

where  $\beta$  is the angle between the magnetic moment and the  $a$ -axis, as shown in Fig. 9. From an examination of (42) it is evident that there are five unknown parameters. However, only three orthogonal  $\gamma$ -ray detectors are required, when both the 712 and 810 keV  $\gamma$ -rays are monitored simultaneously. In general, the experimentally determined average statistical tensors were compared with theoretical calculations, based on a simple molecular field model of the ordered state. However, many body calculations were also performed using the random phase approximation (RPA) to model not only the statistical tensors, but also the elementary excitations of the enhanced antiferromagnetic state (Bleaney *et al.*

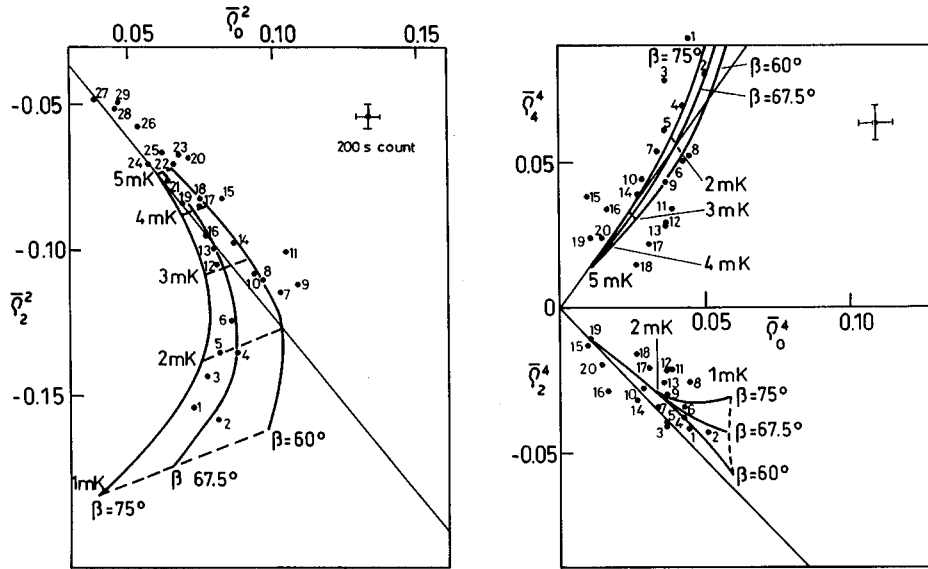


**Fig. 10.** Calculated statistical tensor plots,  $\bar{\rho}_2^2$ ,  $\bar{\rho}_0^2$ ,  $\bar{\rho}_4^4$ ,  $\bar{\rho}_2^4$ , and  $\bar{\rho}_0^4$ , and the measured NO data with  $B_{\text{app}} = 10.0$  mT. The dashed lines indicate the temperature in mK, while  $\beta$  indicates the spin-flop angle in accord with Fig. 9. [After Clark *et al.* (1987).]

1981; Bowden and Clark 1983*a*, 1983*b*; Bowden *et al.* 1986*a*, 1986*b*). In particular, the latter have shown that statistical tensors calculated using spin-wave and related theories, can be well-modelled by a simple effective, but not molecular, field model.

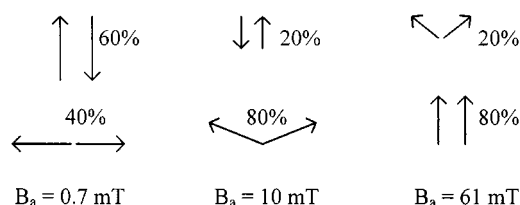


**Fig. 11.** The ‘best-fit model’ for  $\text{HoVO}_4$ , for magnetic fields applied along the  $a$ -axis. [After Clark *et al.* (1987).]

Proceeding in this fashion, Clark *et al.* (1987) were able to provide a surprisingly detailed description of the spin-flop transition in  $\text{HoVO}_4$ . An example of their work can be seen in Fig. 10. Not only were they able to identify the spin-flop, via both second order ( $\bar{\rho}_0^2 - \bar{\rho}_2^2$ ) and fourth order ( $\bar{\rho}_0^4 - \bar{\rho}_2^4, \bar{\rho}_4^4$ ) statistical tensor plots, but also to distinguish between mixed spin-flop and antiferromagnetic/ferromagnetic domains, as summarised in Fig. 11. These results were subsequently interpreted in terms of a pinned domain model, with the pinning ascribed to the presence of Er impurities at about the 400–600 ppm level. Spectroscopic analysis showed Er impurities at 400(12) ppm with no Dy, and calculation showed that a further 200 ppm would be produced by the short lived  $^{166}\text{Ho} \rightarrow \text{Er}$  radioactive decay. To date no NMR or NMRON experiments on Ho isotopes in the ordered regime have been reported. However, the enhanced nuclear ordered state has been probed, indirectly, using  $^{51}\text{V}$  ( $I = \frac{7}{2}$ ) NMR at the vanadium sites (Bleaney *et al.* 1987). Above  $T_N$ , the lowest  $^{51}\text{V}$  NQR resonance ( $\pm \frac{7}{2} \rightarrow \frac{5}{2}$ ) is at 993.4 kHz. When  $\text{HoVO}_4$  was self-cooled to below 5 mK, a dipolar field shift of  $-8.0(5)$  kHz was observed. This is in excellent agreement with the calculated value of  $-8.28$  kHz (8.1 mT). However, rapid heating of the nuclear spins, even with an RF field of only 50 nT, and NMR linewidth problems, precluded a more detailed investigation. This suggests therefore that thermometric  $^{165}\text{Ho}$  NMR investigations are unlikely to be successful, given that the NMR measurement will inject heat directly into the enhanced nuclear spin system.

The  $^{166\text{m}}\text{Ho}$  studies, described above, have been complemented by neutron scattering experiments on an adiabatically self-cooled crystal, to about 3 mK (Suzuki *et al.* 1984*a*, 1984*b*, 1984*c*; Nicklow *et al.* 1985). These authors have confirmed the  $a$ -axis antiferromagnetic structure of  $\text{HoVO}_4$ , using diffraction scans about the (001) position in reciprocal space. In addition, they also witnessed the spin-flop in  $\text{HoVO}_4$ , in applied magnetic fields of about 8 mT.

In summary therefore, NO studies of  $\text{HoVO}_4$ , using in situ radioactive  $^{166\text{m}}\text{Ho}$ , have led to the development of new techniques for the determination of quite complicated spin structures and mixed domains. Indeed, it is fair to say that NO techniques can be used either to rival or complement neutron scattering, as a means of examining the properties of the ordered state, particularly in the mK regime.

## 6. CeVO<sub>4</sub>

Little is known about this compound. From EPR measurements we have  $g_z = 0.864$  and  $g_\perp = 1.503$  (Baker 1995). If we use the set of crystal field parameters for PrVO<sub>4</sub> given in the next section, and adapt them to CeVO<sub>4</sub>, using the appropriate Stevens constants ( $\alpha$ ,  $\beta$ ,  $\gamma$ ), and extrapolated radial expectation values  $\langle r^n \rangle$  from Freeman and Desclaux (1979), we find ( $\mathcal{B}_{20} = -226$ ,  $\mathcal{B}_{40} = -708$ ,  $\mathcal{B}_{44} = -9669 \text{ cm}^{-1}$ ). The resulting, well separated, ground state Kramers doublet is found to be

$$|\psi_g\rangle = \alpha|\pm \frac{5}{2}\rangle + \beta|\mp \frac{3}{2}\rangle, \quad (43)$$

with  $\alpha = 0.713$  and  $\beta = 0.701$ . The calculated values of  $g_z$  and  $g_\perp$  are 0.914 and 1.916, respectively, not far from the EPR results.

Bleaney (1995*a*) has estimated that this compound should order antiferromagnetically at 23 mK, presumably in the  $a$ - $a'$  plane. Since all the stable Ce isotopes have  $I = 0$  spin, there will be no local field arising from fluctuating nuclear moments. So it should be possible to self-demagnetise CeVO<sub>4</sub> well below  $T_N$ .

Clearly, thermometric NMR studies of CeVO<sub>4</sub> are impossible. However, there are several radioactive Ce isotopes which might be employed (see for example Krane 1986).

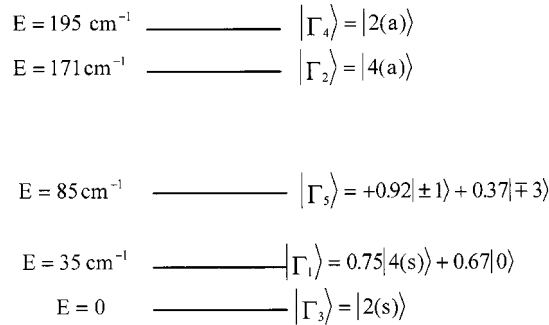


**Fig. 12.** Energy levels and eigenvectors for the Pr<sup>3+</sup> ion in PrVO<sub>4</sub>. [After Nguyen *et al.* (1997).] There are two further levels at 343 and 409 cm<sup>-1</sup> (not shown). The notation  $|2(s, a)\rangle$  is shorthand for  $\sqrt{\frac{1}{2}}[|2\rangle \pm | -2\rangle]$ .

## 7. PrVO<sub>4</sub>

The crystal field levels of the Pr<sup>3+</sup> ion in PrVO<sub>4</sub> have been determined by Nguyen *et al.* (1997) using electronic Raman scattering (ERS) experiments. The energy levels are summarised in Fig. 12. Both the ground state and first excited states are non-magnetic singlets, and there are no Zeeman matrix elements between the ground and first excited states. However, non zero matrix elements  $\langle \Gamma_3 | J_{x,y} | \Gamma_5 \rangle$  do exist between the ground state and second excited state doublet at 85 cm<sup>-1</sup>. Thus PrVO<sub>4</sub> is a weak van Vleck paramagnet. The measured  $g$ -factors are  $g_{||} = 0.0180$  and  $g_\perp = 0.0572$  (Bleaney *et al.* 1977).

NMR measurements in the paramagnetic range 1.6 to 20 K using  $^{141}\text{Pr}$  and  $^{51}\text{V}$  have been reported by Bleaney *et al.* (1977). For  $^{141}\text{Pr}$ , they reported that  $\gamma/2\pi = 24.6$  and  $\gamma_{\perp}/2\pi = 77.6$  (MHz  $\text{T}^{-1}$ ). On comparing these values with the bare moment of  $\gamma_{\parallel}/2\pi = 13.0$  (MHz  $\text{T}^{-1}$ ), it is clear that  $\text{PrVO}_4$  is a weak enhanced nuclear system, both parallel to and perpendicular to the tetragonal  $c$ -axis. So it is likely that this compound will order at a very low temperature  $\sim 10$   $\mu\text{K}$ . The quadrupole parameter  $4P/h$ , which is 13.5 MHz at 1.6 K, is once again made of three contributions: an intra-ionic 4f term, a lattice term and a pseudo-quadrupole interaction.

The NMR work has been complemented by the magnetic measurements of Andronenko *et al.* (1994), in fields of up to 5 T over a temperature range of 4–40 K. These authors give a very similar set of crystal field parameters ( $B_{20} = -77$ ,  $B_{40} = 71$ ,  $B_{60} = -68$ ,  $B_{44} = 970$ ,  $B_{64} = -200$   $\text{cm}^{-1}$ ) at 7 K, but note that they are temperature dependent.

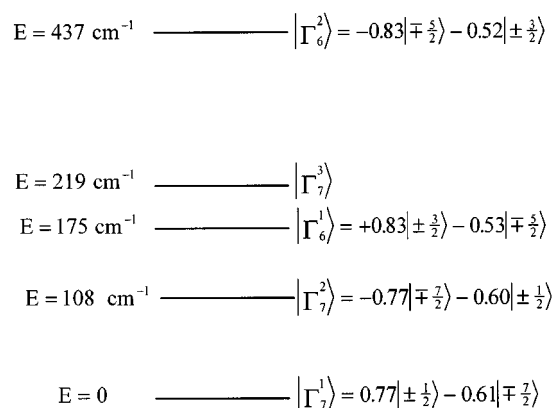


**Fig. 13.** Energy levels and eigenvectors for the  $\text{Nd}^{3+}$  ion in  $\text{NdVO}_4$ . [After Nguyen *et al.* (1997).] The  $|\Gamma_7^3\rangle$  state is a mixture of  $L = 6$  and  $5$  states:  $|\Gamma_7^3\rangle = |-0.98^4 I_{9/2}(\pm \frac{9}{2}) + 0.17^2 H_{9/2}(\pm \frac{9}{2})$ .

## 8. $\text{NdVO}_4$

The crystal field levels of the  $\text{Nd}^{3+}$  ion in concentrated  $\text{NdVO}_4$  have been determined by Nguyen *et al.* (1997) using ERS experiments. The energy levels are summarised in Fig. 13. From EPR experiments on dilute  $\text{Nd}^{3+}$  in  $\text{YVO}_4$ , Ranon (1968) reported that  $g_{\parallel} = 0.915(5)$  and  $g_{\perp} = 2.348(2)$  for the Kramers ground state doublet. Using the ground state assignment given by Nguyen *et al.* (1997) we find  $g_{\parallel} = 1.641$  and  $g_{\perp} = 2.156$ , which differ somewhat from the measurements of Ranon. However, since  $g_{\perp}$  is larger than  $g_{\parallel}$  in both cases, it is likely that  $\text{NdVO}_4$  will order in the  $a$ - $a'$  plane. A set of crystal field parameters for lightly doped  $\text{Nd}/\text{YVO}_4$  has also been given by Tanner and Edelstein (1988).

From the NO point of view,  $^{147}\text{Nd}$  could be used as a radioactive probe (see for example Krane 1986). However, there are two stable Nd isotopes which could also be used for thermometric NMR experiments.

### 9. SmVO<sub>4</sub>

Bleaney (1988, 1995*a*) has given the values of  $g_{\parallel} = 0.506$  and  $g_{\perp} = 0.344$  for this compound. Little is known about this particular vanadate, but Bleaney (1995*a*) has estimated that SmVO<sub>4</sub> should order antiferromagnetically at 43 mK. Few NO measurements using Sm isotopes have been reported (e.g. Krane 1986), but there are plenty of stable isotopes which could be used for thermometric NMR studies.

### 10. EuVO<sub>4</sub>

Europium vanadate has been discussed by Bleaney and Leask (1994) and Bleaney (1995*a*, 1995*b*), who have suggested several experiments such as nuclear orientation, dynamic nuclear orientation, hole-burning, and nuclear acoustic resonance. EuVO<sub>4</sub> differs from all other RE vanadates in that the Eu<sup>3+</sup> 4f<sup>6</sup> (<sup>7</sup>F<sub>0</sub>) ground state spin  $J$  is zero, with the first excited state  $J = 1$ , at  $\sim 360 \text{ cm}^{-1}$  (520 K). Thus at low temperatures EuVO<sub>4</sub> is a van Vleck paramagnet. So the problem reduces to a study of intermixing of the  $J = 0$  and 1 spin states by the hyperfine interactions and applied fields. In practice, intermixing of the  $J = 0$  and 1 levels reduces the stable Eu ( $I = \frac{3}{2}$ ) and <sup>151</sup>Eu ( $I = \frac{3}{2}$ ) and <sup>153</sup>Eu ( $I = \frac{3}{2}$ ) nuclear Zeeman splittings by an appreciable amount, leading to quite low NMR frequencies of a few MHz per Tesla. Such low frequencies will make NMRON experiments difficult, even though there are several Eu isotopes which could be used as probes. In view of this, Bleaney has suggested the use of CeVO<sub>4</sub> as a host, which is expected to order at about  $T_N = 23 \text{ mK}$ . Moreover, because Ce possesses no odd isotopes, it should be possible to self-demagnetise this host to very low temperatures. In this way, it may be possible to orientate the radioactive isotopes Eu<sup>152</sup> ( $I = 3$ ) and <sup>154</sup>Eu ( $I = 3$ ) using quadrupolar alignment, since their overall quadrupolar splittings are estimated to be  $9P/h = 16$  and 20 mK respectively.

### 11. GdVO<sub>4</sub>

Gadolinium vanadate is an easy  $c$ -axis antiferromagnet with a Néel temperature  $T_N$  of 2.495 K (Cashion *et al.* 1970; Metcalfe and Rosenberg 1972*a*). For fields applied along the  $c$ -axis, GdVO<sub>4</sub> exhibits a spin flop at 1.08 T, at 0.5 K. In higher fields the moments close up, in a linear fashion, reaching saturation at 2.92 T. These results can be interpreted in terms of the exchange and anisotropy fields  $B_E$  and  $B_A$ , using a simple mean field model. Within this approximation, the spin-flop field is given by

$$B_{\text{SF}} = \sqrt{B_A(2B_E - B_A)}, \quad (44)$$

whereas the two critical fields required to reach magnetic saturation are given by

$$B_{C\perp} = (2B_E + B_A), \quad B_{C\parallel} = (2B_E - B_A). \quad (45)$$

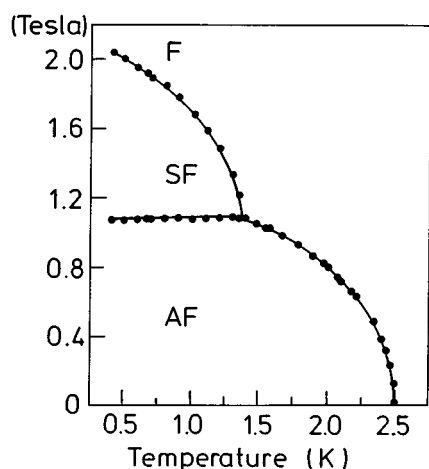


**Fig. 14.** Magnetic phase diagram of  $GdVO_4$  with  $B$  applied along the  $c$ -axis. [After Mangum and Thornton (1971).]

From their measurements, Cashion *et al.* (1970) deduced that  $B_E = 1.275$  T and  $B_A = 0.37$  T respectively.

More detailed magnetic measurements have been reported by Mangum and Thornton (1971) and Colwell *et al.* (1971). The phase diagram from Mangum and Thornton (1971) is reproduced in Fig. 14. These authors also note that the anisotropy associated with the dipole-dipole interactions between the  $Gd^{3+}$  ions is about the same strength as that of the crystal field. So the simple treatment given by Cashion *et al.* (1970) should be modified. However, more recently Abraham *et al.* (1992) have re-examined the interpretation of  $GdVO_4$  results, in the light of their new antiferromagnetic resonant measurements. These authors note that there are two experimental quantities which need no correction for demagnetisation field: namely the antiferromagnetic resonance condition in zero applied field:

$$B_{AFR} = \sqrt{B_A(2B_E + B_A)}, \tag{46}$$

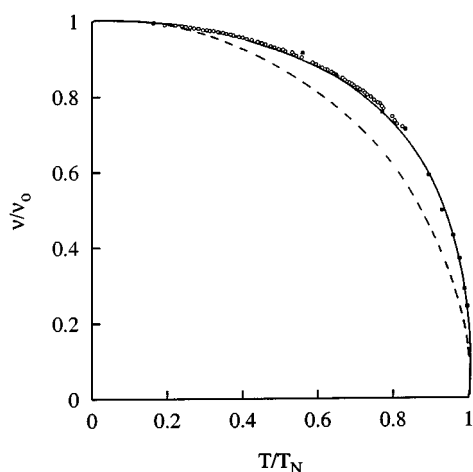


**Fig. 15.** Reduced magnetic hyperfine field at the  $^{51}V$  nucleus in  $GdVO_4$ , as measured by NMR. [After Bleaney *et al.* (1988).] The dashed curve is the molecular field prediction for  $S = \frac{7}{2}$ . The solid curve is the reduced magnetisation, as determined from the parallel susceptibility  $\chi_{||}$  of Cashion *et al.* (1970) (see text).

and the spin-flop field of (44). Using the measured quantities of 1.22 and 1.08 T (extrapolated to  $T = 0$  K), they find  $B_E = 1.655$  T and  $B_A = 0.401$  T, rather higher than those of Cashion *et al.* (1970). But if these new values are used to predict the two critical fields for magnetic saturation, they find  $B_{C\perp} = 3.71$  T and  $B_{C\parallel} = 2.90$  T, much higher than the measured values of 2.92 and 2.18 T, respectively, of Cashion *et al.* (1970). Given these discrepancies, Abraham *et al.* (1992) concluded that it is difficult to obtain an overall self-consistent analysis for  $\text{GdVO}_4$ , within the mean field model.

Further evidence for the breakdown of the mean field approach can be gleaned from the  $^{51}\text{V}$  NMR results of Bleaney *et al.* (1981*b*). These authors have presented an astonishingly accurate determination of the temperature dependence of the magnetic hyperfine field at the  $^{51}\text{V}$  site, down to 0.48 K. Their results are summarised in Fig. 15, where it will be seen that the reduced magnetic hyperfine field  $v(T)/v(T = 0 \text{ K})$ , plotted against the reduced temperature ( $T/T_N$ ), does not agree with the molecular field prediction for  $S = \frac{7}{2}$ . For the temperature region investigated Bleaney *et al.* found

$$\begin{aligned} v/v_0 &= 1 - 0.0443T^2 - 0.00492T^4 \\ &= 1 - 0.2759(T/T_N)^2 - 0.1908(T/T_N)^4. \end{aligned} \quad (47)$$

At very low temperatures, (47) agrees well with the  $T^2$  low temperature prediction of spin-wave theory, if the energy gap in the spin-wave dispersion curve is zero. However, the presence of an anisotropy field  $B_A$  suggests that it is unlikely that the energy gap in the spin-wave spectrum will be zero.

Bleaney *et al.* (1981) also noted that very good agreement with their NMR data can be obtained, if they use the measured parallel susceptibility  $\chi_{\parallel}(T)$  of Cashion *et al.* (1970) to deduce the reduced magnetisation, using the method of Hornreich and Shtrikman (1967). Since the latter is firmly based on (i) thermodynamic arguments and (ii) underpinned by the Callen and Shtrikman (1965) result (which enables moments  $\langle J_z^n \rangle$  to be generated in agreement with many body predictions), good agreement between the two, at first sight dissimilar, sets of data can be anticipated. Conversely, however, this result implies that a more sophisticated model, other than the simple mean field model, will be required to provide a consistent magnetic framework for  $\text{GdVO}_4$ .

Mössbauer  $^{165}\text{Gd}$  86.5 keV measurements on  $\text{GdVO}_4$  have been reported by Cook and Cashion (1979), down to 0.4 K. Their results were used, primarily, to probe the temperature dependence of the reduced magnetic hyperfine field directly at the Gd site. They found

$$\frac{B(T)}{B(0)} = 1 - 0.567 \left( \frac{T}{T_N} \right)^3, \quad (48)$$

from  $T = 0$  to  $0.85 T_N$ , rather different from that of Bleaney *et al.* (1981*b*). From a comparison of the two types of experiment, it is clear that the  $^{51}\text{V}$  NMR results are more accurate than the  $^{165}\text{Gd}$  86.5 keV Mössbauer measurements. Nevertheless, the Mössbauer results do have an advantage in that they probe the Gd site directly.

No NMR or NMRON studies on the Gd sites in  $\text{GdVO}_4$  have been reported. However, thermometric NMR methods using  $^{155}\text{Gd}$  and  $^{157}\text{Gd}$  might be used to complement the phase diagram measurements of Magnum and co-workers (1971) in the mK regime. Note that (i) the Gd resonances will be much lower in frequency, because of the S-state nature of the  $\text{Gd}^{3+}$  ion, (ii) the NMR enhancement factor  $\eta$  will vary considerably on traversing the magnetic phase boundaries, and (iii) it should be possible to extract information concerning spin directions from the measured quadrupole interaction. In addition, we note that  $^{51}\text{V}$  NMR measurements and/or  $^{165}\text{Gd}$  86.5 keV Mössbauer measurements could also be used to probe the magnetic phase boundaries, if required.

It should also be possible to detect antiferromagnetic resonance in  $\text{GdVO}_4$ , via thermometric means. In zero applied field, the antiferromagnetic resonance occurs at 30.61(2) GHz, at 1.36 K (Abraham *et al.* 1992).

Finally we note that the large neutron cross sections associated with  $^{155}\text{Gd}$  and  $^{157}\text{Gd}$  will preclude neutron studies on samples prepared with natural Gd abundance.

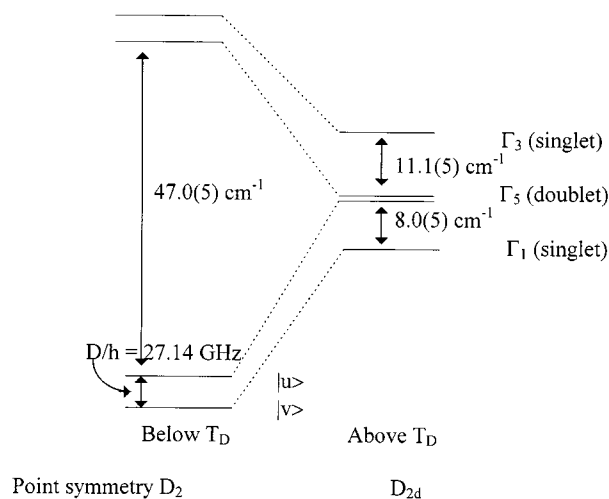


**Fig. 16.** Low lying electronic levels of  $\text{Tb}^{3+}$  in  $\text{TbVO}_4$ , before and after the Jahn–Teller distortion. [After Bleaney *et al.* (1997).]

## 12. $\text{TbVO}_4$

The cooperative Jahn–Teller distortion in  $\text{TbVO}_4$  has been put at 33.1 K by Wells and Wornick (1972) and 32.8 K by Harley *et al.* (1980). The distortion is of the  $B_{2g}$  type. The resultant low lying energy levels of the  $\text{Tb}^{3+}$ , above and below the Jahn–Teller distortion, are shown in Fig. 16. These are taken from Gehring *et al.* (1971, 1976) and Bleaney *et al.* (1997). The two low lying singlets, below  $T_D$ , are given by

$$|u\rangle = 0.367|5(a)\rangle - 0.714|1(a)\rangle + 0.597|3(a)\rangle, \quad |v\rangle = 0.957|\Gamma_3\rangle + 0.290|\Gamma_1\rangle, \quad (49)$$

where  $|5(s, a)\rangle$  etc. is shorthand notation for

$$|5(s, a)\rangle = -\sqrt{\frac{1}{2}}[|5\rangle \pm |-5\rangle], \quad (50)$$

respectively, and

$$|\Gamma_3\rangle = 0.164|6(a)\rangle - 0.986|2(a)\rangle, \quad (51)$$

$$|\Gamma_1\rangle = 0.708|4(s)\rangle - 0.706|0\rangle. \quad (52)$$

These two singlets  $|v\rangle$  and  $|u\rangle$  may be treated as a non-Kramers  $S = \frac{1}{2}$  doublet, with an energy separation  $D$ . From EPR experiments at 4.2 K,  $D$  is found to be 27.14 GHz (Bleaney *et al.* 1997). EPR experiments have shown that the  $g$ -factor for the [110] and  $[1\bar{1}0]$  directions is 16.3 for  $g\mu_B B \gg D$ , and zero for the other two directions (Gehring *et al.* 1971). Thus the magnetic moments will be constrained to lie along the [110] or equivalent axes.

Because  $\text{TbVO}_4$  is an interesting example of two level singlet magnetism, Gehring *et al.* (1976) have discussed its magnetic properties both within the molecular field model and the random phase approximation (RPA). However, as noted by Bleaney *et al.* (1997), no account was taken of the magnetic hyperfine interaction which gives rise to large enhanced moments. These are estimated to be  $\pm 2.516 \mu_B$  for the  $m = \pm \frac{3}{2}$  and  $\pm 0.876 \mu_B$  for the  $m = \pm \frac{1}{2}$   $^{159}\text{Tb}$  nuclear states. Thus the Néel temperature  $T_N$  is likely to be higher than that expected on just the basis of dipolar and exchange fields alone. Further, in addition, to the enhanced nuclear moments, the intra-ionic quadrupole interaction of equation (5), possesses non-zero matrix elements  $\langle v|\mathcal{H}_Q|v\rangle$ ,  $\langle u|\mathcal{H}_Q|u\rangle$ , and  $\langle v|\mathcal{H}_Q|u\rangle$  for the two singlets in question. Thus the full NMR spectrum of this compound is likely to be far from trivial. Clearly  $\text{TbVO}_4$  would be an excellent candidate for (i) thermometric NMR studies using 100% abundant  $^{159}\text{Tb}$  ( $I = \frac{3}{2}$ ) and (ii) NMRON experiments using radioactive  $^{160}\text{Tb}$ . It may also be worth while carrying out EPR/ENDOR type experiments in the 30 GHz range (perhaps thermometrically) to detect the hyperfine structure on the EPR line. Since most NMRON experiments, using  $^3\text{He}/^4\text{He}$  dilution refrigerators, have been carried out at frequencies below  $\sim 1$ – $2$  GHz, this would represent something of a challenge. A tuned NMR cavity operating at 6 GHz at 1 K has been discussed by Carboni *et al.* (1989). Finally, there is a need to generalise the theoretical work of Gehring *et al.* (1976), to include both the Tb magnetic and quadrupole hyperfine interactions.

### 13. Antiferromagnetic $\text{DyVO}_4$

From EPR measurements on  $\text{Dy}^{3+}$  doped  $\text{YVO}_4$  at 1.8 and 4.2 K, it is known that the ground state of the  $\text{Dy}^{3+}$  ( $J = \frac{15}{2}$ ) ion is an expected Kramers doublet, with  $g_\perp = 9.903(5)$  and  $g_\parallel = 1.104(1)$  (Ranon 1968). Further, from experiments on 100% concentrated  $\text{DyVO}_4$ , Cooke *et al.* (1970, 1971) gave  $g_a = 9.50(25)$ ,  $g_{a'} \leq 0$ ,  $g_c = 0.25$ , within a fictitious spin doublet. Thus  $\text{DyVO}_4$  can be considered 'Ising-like', in that the Dy magnetic moments must develop along the  $\pm a$  axis. However, because of the very strong magnetic anisotropy, the orthorhombic  $a$  or  $a'$  axes can be interchanged, by application of external magnetic fields.

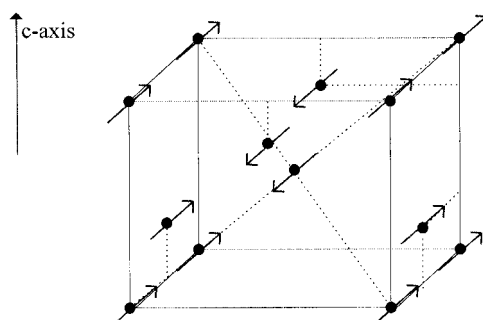


Fig. 17. Antiferromagnetic structure in  $\text{DyVO}_4$  at 1.85 K. [After Will and Schäfer (1971).]

Below the Jahn–Teller distortion temperature of  $14.0(5)$  K the crystal symmetry changes from tetragonal to orthorhombic  $I_{\text{mma}} - D_{2\text{h}}^{28}$  (i.e.  $B_{1\text{g}}$  type). Below  $T_{\text{N}} = 3.066(2)$  K,  $\text{DyVO}_4$  adopts the antiferromagnetic state shown in Fig. 17. It is also known that there is a spin-flip transition to a ferromagnetic state in a field of  $0.21$  T (Ellis *et al.* 1971).

The measured magnetic moment along the  $a$ -axis at  $1.85$  K is  $9.0 \mu_{\text{B}}$ , with an extrapolated value of  $9.5 \mu_{\text{B}}$  at  $0$  K. Thus the magnetic moment is close to the maximum of  $10 \mu_{\text{B}}$  available to the  $\text{Dy}^{3+}$  ion. To the author's knowledge no NMR, NMRON or Mössbauer measurements have been made on this compound below  $1.85$  K. However, this compound would be an excellent candidate for thermometric NMR detection of the stable isotopes  $^{161}\text{Dy}$  and  $^{163}\text{Dy}$ .

Finally, given that  $\text{DyVO}_4$  magnetises preferentially along either the  $a$  or  $a'$  axes, it is possible that this compound might be a candidate for magnetic refrigeration in applied magnetic fields, in a fashion similar to  $\text{DyPO}_4$  and  $\text{YbVO}_4$ .

#### 14. Antiferromagnetic $\text{ErVO}_4$

EPR experiments on Er doped  $\text{YVO}_4$  reveal that the ground state of the  $\text{Er}^{3+}$  ion is an expected Kramers doublet with  $g_{\parallel} = 3.544(5)$  and  $g_{\perp} = 7.085(5)$  (Ranon 1968). These values are in reasonable accord with  $g_{\parallel} = 3.85(3)$  and  $g_{\perp} = 8.5(5)$  for concentrated  $\text{ErVO}_4$  (Staude 1972). There are two higher doublets at  $43.6$  and  $45.4 \text{ cm}^{-1}$ , which can be appreciably admixed into the ground state by the application of magnetic fields.

At temperatures below  $0.4(1)$  K,  $\text{ErVO}_4$  orders antiferromagnetically (Metcalf and Rosenberg 1972*b*). Not much is known about the magnetic structure adopted by the Er moments, but it is possible that it will be similar to that observed in  $\text{DyVO}_4$ . It is also known that  $\text{ErVO}_4$  exhibits a metamagnetic transition to the paramagnetic phase, in fields of about  $0.27$  T, applied along the  $c$ -axis. To the author's knowledge no NMR, NMRON, or neutron scattering results are available for this compound. However, it is clear that  $\text{ErVO}_4$  would be an interesting candidate for the determination of magnetic spin structures, in applied magnetic fields.

#### 15. Antiferromagnetic $\text{TmVO}_4$

From EPR studies on dilute  $\text{Tm}^{3+}$  in  $\text{YVO}_4$ , it is known that the ground state of the  $\text{Tm}^{3+}$  ion is a degenerate (non-Kramers) doublet with a singlet

state some  $53.8 \text{ cm}^{-1}$  above the ground state (Knoll 1971). The ground state is predominantly  $|J_z = \pm 5\rangle$ , with a  $g_{\parallel}$  of 9.96. Cooke *et al.* (1972) reported that similar behaviour occurs in  $\text{TmVO}_4$  above the Jahn–Teller distortion temperature of 2.1 K. Below the Jahn–Teller distortion, which is of the  $B_{2g}$  type, the doublet splits into two non-magnetic singlets separated by  $\Delta(T)$ . This splitting can be measured by applying magnetic fields along the  $c$ -axis. When the Zeeman splitting of the doublet state exceeds that of the crystalline distortion, the crystal will ‘undistort’. The critical field is given by

$$g_{\parallel}\mu_B B_C = k\Delta(T). \quad (53)$$

In practice, it is found that the splitting  $\Delta(T)$  is well described by molecular field theory, with  $\Delta(T=0) = 0.63 \text{ T}$ .

A precise study of both the  $^{169}\text{Tm}$  and  $^{51}\text{V}$  NMR resonances in  $\text{TmVO}_4$ , above and below  $T_D$  to 1.5 K, has been reported by Bleaney and Wells (1980). In addition, these authors have given an accurate value for the Jahn–Teller distortion temperature of  $T_D = 2.156(6) \text{ K}$ . Above  $T_D$  they give the approximate ground and first excited states shown in Fig. 18.

$$\begin{aligned} E = 538 \text{ cm}^{-1} & \text{—————} |\Gamma\rangle = 0.66|0\rangle + 0.54[|4\rangle + |-4\rangle] \\ E = 0 & \text{—————} |\Gamma\rangle = 0.92|\pm 5\rangle - 0.37|\pm 1\rangle + 0.12|\mp 3\rangle \end{aligned}$$

**Fig. 18.** Approximate wavefunctions for the  $\text{Tm}^{3+}$  ion in  $\text{TmVO}_4$ , above the Jahn–Teller distortion temperature. [After Bleaney and Wells (1980).]

Within the non-Kramers ground state doublet, it is easy to show that the response of the  $\text{Tm}^{3+}$  ion to an applied magnetic field  $B$  is second order in  $B$ . The situation is more difficult below  $T_D$ . Bleaney and Wells (1980) have used the same wavefunctions as those shown in Fig. 17, but with an energy separation of  $\Delta$ . When the magnetic hyperfine interaction is switched on, enhanced nuclear moments, with  $K \sim 774$ , appear along the  $c$ -axis, with little in the  $a$ – $b$  plane. Thus if  $\text{TmVO}_4$  orders magnetically, it will be along the  $c$ -axis. Bleaney and Wells have given an estimate for the Néel temperature of 0.25–0.28 mK.

$\text{TmVO}_4$  has been examined in the mK range, using SQUID magnetometry (Suzuki *et al.* 1980, 1981). These authors have shown that the  $c$ -axis is the preferred direction of magnetisation ( $\chi_c/\chi_a = 4.0/0.095$ ), and that the  $c$ -axis magnetic susceptibility is relatively large, on account of the large NMR enhancement for this axis. From self-cooled adiabatic demagnetisation experiments down to  $\sim 100 \mu\text{K}$ , it was found that the susceptibility  $\chi_c$  shows Curie–Weiss behaviour, with a Weiss intercept of  $139 \mu\text{K}$ . However, unlike  $\text{HoVO}_4$  no magnetic ordering was observed above  $100 \mu\text{K}$ . Thus, the ordering temperature must be much lower than the lower estimate of  $250 \mu\text{K}$  given by Bleaney and Wells (1980). Nevertheless, if dipolar ordering is predominant, the resultant magnetic structure will probably be very similar to that observed in  $\text{YbVO}_4$  (see Fig. 2).

Although no NMR resonances were reported by Suzuki *et al.* (1980, 1981), a special study of spin-lattice relaxation times was made using the paramagnetic relaxation method. This revealed that  $T_1$  could be fitted well with the formula

$$T_1^{-1} = 1.4 \times 10^4 \exp(-\Delta/2kT) + 1.6 \times 10^2 \text{ T}, \quad (54)$$

where  $\Delta = 3.0 \text{ cm}^{-1}$ . The precise origin of these terms is a matter for debate, but it should be noted that the spin-lattice relaxation rate is extremely rapid for an insulator, being  $\sim 10^{-2} \text{ s}$  at 100 mK. This feature is probably due to the large NMR enhancement factor  $K = 774$ .

In summary, no NMR, Mössbauer, or neutron results are available for this compound, in the ordered regime. Perhaps the most interesting feature of  $\text{TmVO}_4$  is that the Jahn–Teller distortion can be ‘undone’ by applying quite modest applied fields along the  $c$ -axis. Since there is an appreciable amount of heat released/taken up during this transition (Cooke *et al.* 1972), and the spin lattice relaxation time is relatively rapid (Suzuki *et al.* 1980, 1981), it should be possible to use this compound as (i) a magnetic refrigerator for reaching temperatures below 1 mK, and (ii) to reset perturbed nuclear energy levels by applying the critical field  $B_C$ . Clearly, thermometric NMR experiments, carried out using an external  $^{60}\text{Co}$  thermometer attached to the copper cold finger of the  $^3\text{He}/^4\text{He}$  dilution refrigerator, would be of interest.

## 16. Discussion and Conclusions

In this review, an attempt has been made to collate and discuss the known properties of the rare earth vanadates, in the low temperature regime. It is apparent that much work remains to be done, not only for the vanadates, but also for the phosphates and the arsenates. Of the fourteen vanadates, only two have been studied in any depth:  $\text{HoVO}_4$  and  $\text{YbVO}_4$ . Nevertheless, these two compounds, which are examples of singlet state enhanced magnetism, and a magnetic Kramers doublet, respectively, have been used to generate a surprising amount of novel physics. In particular,  $^{166\text{m}}\text{Ho}$  NO studies in  $\text{HoVO}_4$  have ushered in new ways of determining magnetic structures, offering a valuable alternative to neutron scattering. On the other hand, NO studies on  $\text{YbVO}_4$  have paved the way for thermometric NMR studies on stable isotopes, as well as allowing a new mechanism for intermediate state orientation to be identified. Indeed, the experience gained with  $\text{YbVO}_4$ , suggests that before any NMRON experiments are carried out, thermometric NMR on the stable isotopes should be performed, before introducing radioactive isotopes into the crystal by, say, neutron irradiation. This approach not only avoids introducing radiation damage, but will also make NMR searches easier. Because of the homogeneously broadened linewidths, associated with concentrated isotopes, fewer frequency steps will be required to locate a given resonance. But more importantly, it avoids introducing unwanted impurities into the sample, such as  $\text{Er}^{3+}$  in  $\text{HoVO}_4$  and  $\text{Lu}^{4+}$  in  $\text{YbVO}_4$ .

Finally, we remark that in this review many experiments have been suggested en-route. But perhaps  $\text{TbVO}_4$  stands out as an interesting candidate for both thermometric NMR on the 100% abundant isotope  $^{159}\text{Tb}$ , and NO and NMRON studies, using in situ radioactive  $^{160}\text{Tb}$ . Moreover, since  $\text{TbVO}_4$  is an enhanced

nuclear system, it will be necessary to determine the Tb nuclear hyperfine parameters, since they will play a role in driving the antiferromagnetic transition at 0.61 K. Such experiments, will also provide a necessary precursor to more theoretical work on the singlet–singlet magnetism of TbVO<sub>4</sub>, driven in part by the presence of enhanced nuclear moments.

### Acknowledgments

The author gratefully acknowledges the help of all his collaborators, but in particular B. Bleaney, N. J. Stone, D. H. Chaplin, W. D. Hutchison and M. J. Prandolini. Thanks are also due to B. Bleaney and L. Boatner who supplied preprints of work prior to publication.

### References

- Abragam, A., and Bleaney, B. (1970). ‘Electron Paramagnetic Resonance of Transition Ions’ (Clarendon Press: Oxford).
- Abragam, A., and Bleaney, B. (1983). *Proc. R. Soc. London A* **387**, 221–56.
- Abraham, M. M., Baker, J. M., Bleaney, B., Pfeffer, J. Z., and Wells, M. R. (1992). *J. Phys. D* **4**, 5443–46.
- Allsop, A. L., Bleaney, B. (FRS), Bowden, G. J., Nambudripad, N., Stone, N. J., and Suzuki, H. (1980). *Proc. R. Soc. London A* **372**, 19–31.
- Allsop, A. L., Bowden, G. J., Clark, R. G., and Stone, N. J. (1984a). XX11 Congress Ampere, Zurich, pp. 293–4.
- Allsop, A. L., Bowden, G. J., Nambudripad, N., and Stone, N. J. (1979). *Phys. Rev. B* **20**, 359–63.
- Allsop, A. L., Bowden, G. J., Nambudripad, N., Stone, N. J., and Suzuki, H. (1981). *Hyperfine Interact.* **9**, 849–54.
- Allsop, A. L., de Araujo, M., Bowden, G. J., Clark, R. G., and Stone, N. J. (1984b). *J. Phys. C* **17**, 915–37.
- Andronenko, R. R., Andronenko, S. I., and Bazhan, V. A. (1994). *Phys. Solid State (Sov. Phys.)* **36**, 1302.
- Andronenko, S. I., Bazhan, V. A., Ioffe, V. A., and Udalov, Yu P. (1985). *Phys. Solid State (Sov. Phys.)* **3**, 379–81.
- Baker, J. M. (1995). private communication (see Bleaney 1995a).
- Battison, J. E., Kasten, A., Leask, M. J. M., and Lowry, J. B. (1975). *Phys. Lett. A* **55**, 173.
- Battison, J. E., Kasten, A., Leask, M. J. M., and Lowry, J. B. (1977). *J. Phys. C* **10**, 323–32.
- Benoit, A., Flouquet, J., and Steyart, W. A. (1972). *Nucl. Phys. A* **197**, 1092–7.
- Bleaney, B. (1972). In ‘Magnetic Properties of Rare Earth Metals’ (Ed. R. J. Elliott), p. 383.
- Bleaney, B. (1980). *Proc. R. Soc. London A* **370**, 313–30.
- Bleaney, B. (1995a). *Proc. R. Soc. London A* **450**, 711–7.
- Bleaney, B. (1995b). *Proc. R. Soc. London A* **450**, 719–22.
- Bleaney, B., and Leask, M. J. M. (1994). In ‘NMR and More, in Honour of Anatole Abragam, 73’, Les Editions de Physique Les Ulis, pp. 73–80.
- Bleaney, B., and Wells, M. R. (1980). *Proc. R. Soc. London* **370**, 131–53.
- Bleaney, B., Bowden, G. J., and Clark, R. G. (1981). *J. Phys. C* **15**, 1663–83.
- Bleaney, B., Clark, R. G., Gregg, J. F., Roinel, Y., and Stone, N. J. (1987). *J. Phys. C* **20**, 3175–86.
- Bleaney, B., Cooke, A. H., Robinson, F. N. H., and Wells, M. R. (1976). *Physica B* **86–88**, 1145 (XIX Congress Ampere, Heidelberg).
- Bleaney, B., de Oliveira, A. C., Wanklyn, B., and Wells, M. R. (1981a). *Phys Lett. A* **84**, 32–5.
- Bleaney, B., de Oliveira, A. C., and Wells, M. R. (1981b). *J. Phys. C* **14**, 505–8.
- Bleaney, B., de Oliveira, A. C., and Wells, M. R. (1982a). *J. Phys. C* **15**, 5275–91.
- Bleaney, B., de Oliveira, A. C., and Wells, M. R. (1982b). *J. Phys. C* **15**, 5305–19.
- Bleaney, B., Gregg, J. F., and Wells, M. R. (1982d). *J. Phys. C* **15**, L349–52
- Bleaney, B., Gregg, J. F., de Oliveira A. C., and Wells, M. R. (1982e). *J. Phys. C* **15**, 5293–303.

- Bleaney, B., Gregg, J. F., Hansen, P., Huan, C. H. A., Lazzouni, M., Leask, M. J. M., Morris, I. D., and Wells, M. R. (1988). *Proc. R. Soc. London A* **416**, 63–73.
- Bleaney, B., Pfeffer, J. Z., and Wells, M. R. (1997). *J. Phys. C* **9**, 7469–75.
- Bleaney, B., Robinson, F. N. H., and Wells, M. R. (1978). *Proc. R. Soc. London A* **362**, 179–94.
- Bleaney, B., Robinson, F. N. H., Smith, S. H., and Wells, M. R. (1977). *J. Phys. C* **10**, L385–8.
- BlinStoyale, R. J., and Grace, M. A. (1957). In 'Handbuch der Physik XLII' (Ed. S. Flugge), pp. 555–610 (Springer: Berlin).
- Bowden, G. J., and Clark, R. G. (1983a). *J. Phys. C* **16**, 3305–27.
- Bowden, G. J., and Clark, R. G. (1983b). *J. Phys. C* **16**, 1089–98.
- Bowden, G. J., Campbell, I. A., Nambudripad, N., and Stone, N. J. (1979). *Phys. Rev. B* **20**, 352–8.
- Bowden, G. J., Martin, J. P. D., and Oitmaa, J. (1986a). *J. Phys. C* **19**, 551–61.
- Bowden, G. J., Oitmaa, J., and Martin, J. P. D. (1986b). *J. Phys. C* **19**, 155–61.
- Callen, H. B., and Shriktman, S. (1965). *Solid State Commun.* **3**, 5.
- Carboni, C., McKenzie, I. S., and McCausland, M. A. H. (1989). *Hyperfine Interact.* **51**, 1139.
- Cashion, J. D., Cooke, A. H., Hoel, L. A., Martin, D. M., and Wells, M. R. J. (1970). *J. de Phys. C* **6**, 417–26.
- Clark, R. G., Allsop, A. L., Stone, N. J., and Bowden, G. J. (1987). *J. Phys. C* **20**, 797–814.
- Colwell, J. H., Mangum, B. W., and Thornton, D. D. (1971). *Phys. Rev. B* **3**, 3855.
- Cook, D. C., and Cashion, J. D. (1979). *J. Phys. C* **12**, 605–13.
- Cooke, A. H., Ellis, C. J., Gehring, K. A., Leask, M. J. M., Martin, D. M., Wanklyn, B. M., Wells, M. R., and White, R. L. (1970). *Solid State Commun.* **8**, 689–92.
- Cooke, A. H., Martin, D. M., and Wells, M. R. (1971). *Solid State Commun.* **9**, 519–22.
- Cooke, A. H., Swithenby, S. J., and Wells, M. R. (1972). *Solid State Commun.* **10**, 265–8.
- CRC Handbook of Chemistry and Physics (76<sup>th</sup> Edition) (1995–96).
- CRC Handbook of Spectroscopy, Vol. 13 (1981).
- Daniels, J. M., and Misra, S. K. (1966). *Can. J. Phys.* **44**, 1965–84.
- Davaa, S., Kracikova, T. I., Finger, M., Tsupko-Sitnikov, V. M., and Pavlov, V. N. (1987). *Sov. J. Nucl. Phys.* **45**, 387–401.
- Elliott, R. J., Harley, R. T., Hayes, W., and Smith, S. R. P. (1972). *Proc. R. Soc. London A* **328**, 217–66.
- Ellis, C. J., Gehring, K. A., Leask, M. J. M., and White, R. L. (1971). *J. de Phys. (Colloque C1 au n° 2-3, Tome 32)*, C1–1024–5.
- Freeman, A. J., and Desclaux, J. P. (1979). *J. Magn. Magn. Mater.* **12**, 11–21.
- Fuess, H., and Kallel, K. J. (1972). *Solid. State. Chem.* **5**, 11.
- Gehring, G. A., and Gehring, K. A. (1975). *Rep. Prog. Phys.* **38**, 1–89.
- Gehring, G. A., Kahle, H. G., Nagele, W., Simon, A., and Wunchner, W. (1976). *Phys. Stat. Solidi (b)* **74**, 297.
- Gehring, G. A., Malozemoff, A. P., Staude, W., and Tyte, R. N. (1971). *Solid State Commun.* **9**, 511–14.
- Hamilton, W. D. (Ed). (1975). 'The Electromagnetic Interaction in Nuclear Spectroscopy' (North Holland: Amsterdam).
- Harley, R. T., Lyons, K. B., and Fleury, P. A. (1980). *J. Phys. C* **13**, L447–53.
- Haroutunian, R., Meyer, M., Berkes, I., and Marest, G. (1980). *Hyperfine Interact.* **8**, 41–58.
- Hodges, J. A. (1983). *J. de Phys.* **44**, 833–9.
- Hornreich, R. M., and Shriktman, S. (1967). *Phys. Rev. B* **8**, 408–10.
- Hutchings, M. T. (1965). *Solid State Phys.* **16**, 227–73.
- Hutchison, W. D., Prandolini, M. J., Chaplin, D. H., and Bowden, G. J. (1997). unpublished.
- Hutchison, W. D., Prandolini, M. J., Chaplin, D. H., Bowden, G. J., and Bleaney, B. (1996). Low Temperature Conference LT21, Prague, *Czech. J. Phys. (Suppl. S4)* **46**, 2151–2.
- Kassman, A. J. (1970). *J. Chem. Phys.* **53**, 4118.
- Kazei, Z. A., and Popov, Yu F. (1994). *Solid State Phys. (Sov. Phys.)* **36**, 1146–49.
- Knoll, K. D. (1971). *Phys. Stat. Solidi (b)* **45**, 553–9.
- Koonce, C. S., Mangum, B. W., and Thornton, D. D. (1971). *Phys. Rev. B* **4**, 4054–69.
- Krane, K. S. (1986). In Stone and Postsma (Ed.) (1986), p. 71.
- Louasmaa, O. V. (1974). 'Experimental Principles and Methods below 1K' (Academic: New York).

- McCausland, M. A. H., and McKenzie, I. S. (1979). *Adv. Phys.* **28**, 305–456.
- Mangum, B. W., and Thornton, D. D. (1971). AIP Conference Proceedings, Magnetism and Magnetic Materials, Vol. 5, pp. 311–5.
- Metcalfe, M. J., and Rosenberg, H. M. (1972a). *J. Phys. C* **5**, 459–73.
- Metcalfe, M. J., and Rosenberg, H. M. (1972b). *J. Phys. C* **5**, 474–80.
- Nguyen, A. D., Murdoch, K., Edelstein, N., Boatner, L. A., and Abraham, M. M. (1997). *Phys. Rev. B* **56**, 794–87.
- Nicklow, R. M., Moon, R. M., Kawarazaki, S., Kunitomi, N., Susuki, H., and Ohtsuka, T. (1985). *J. Appl. Phys.* **57**, 3784–8.
- Nipko, J. C., Loong, C. K., Kern, S., Abraham, M. M., and Boatner, L. A. (1997). *J. Alloys Compounds* **250**, 569.
- Prandolini, M. J., Hutchison, W. D., Chaplin, D. H., Bowden, G. J., and Bleaney, B. (1997). Contributed paper to ICM 1997, Cairns, Australia.
- Radhakrishna, P., Hammann, J., and Pari, P. (1981). *J. Magn. Magn. Mater.* **23**, 254–6.
- Ranon, U. (1968). *Phys. Lett. A* **28**, 228–9.
- Skanthakumar, S., Loong, C. K., Soderholm, L., Abraham, M. M., and Boatner, L. (1995). *Phys. Rev. B* **51**, 12451–57.
- Staude, W. (1972). as reported in Metcalfe and Rosenberg (1972b).
- Stewart, G. A. (1994). *Mater. Forum* **18**, 177–93.
- Stone, N. J. (1989). *Hyperfine Interact.* **49**, 103–28.
- Stone, N. J., and Postma, H. (Eds) (1986). ‘Low Temperature Orientation’ (North Holland: Amsterdam).
- Strohm, W. W., and Sapp, R. C. (1963). *Phys. Rev.* **132**, 207–14.
- Suzuki, H., and Masuda, Y. (1984). *Solid State Phys. (Japan)* **19**, 660–9.
- Suzuki, H., Inoue, T., and Ohtsuka, T. (1981). *Physica B* **107**, 563–4.
- Suzuki, H., Inoue, T., Higashino, Y., and Ohtsuka, T. (1980). *Phys. Lett. A* **77**, 185–8.
- Suzuki, H., Nambudripad, N., Bleaney, B., Allsop, A. L., Bowden, G. J., Campbell, I. A., and Stone, N. J. (1978). Low Temperature Conference No. 15, *J. de Phys. (Colloque C6, Suppl. 8)*, **39**, 800–2.
- Suzuki, H., Ohtsuka, T., Kawarazakai, S., Kunitomi, N., Moon, R. M., and Nicklow, R. M. (1984a). Proc. 17th Conf. on Low Temperature Physics, Karlsruhe, Vol. 1, pp. 17–18.
- Suzuki, H., Ohtsuka, T., Kawarazakai, S., Kunitomi, N., Moon, R. M., and Nicklow, R. M. (1984b). *Solid. State Commun.* **49**, 1157–60
- Tanner, P., and Edelstein, N. (1988). *Chem. Phys. Lett.* **152**, 140.
- Turrell, B. G. (1986). In Stone and Postma (Eds), pp. 475–526.
- Wäppling, R., Karlsson, E., Carlsson, G., Pernestal, K., and Bajaj, M. M. (1973). *Phys. Scripta* **8**, 73–80.
- Wells, M. R., and Worsnik, R. D. (1972). *Phys. Lett. A* **42**, 269–71.
- Will, G., and Schäfer, W. (1971). *J. Phys. C* **4**, 811–9.
- Wright, J. C., Moos, H. W., Colwell, J. H., Mangum, B. W., and Thornton, D. D. (1971). *Phys. Rev. B* **3**, 843–57.
- Wybourne, B. G. (1965). ‘Spectroscopic Properties of Rare Earths’ (Wiley: New York).
- Wyckoff, R. W. (1965). ‘Crystal Structures’, Vol. 3 (Interscience: New York).